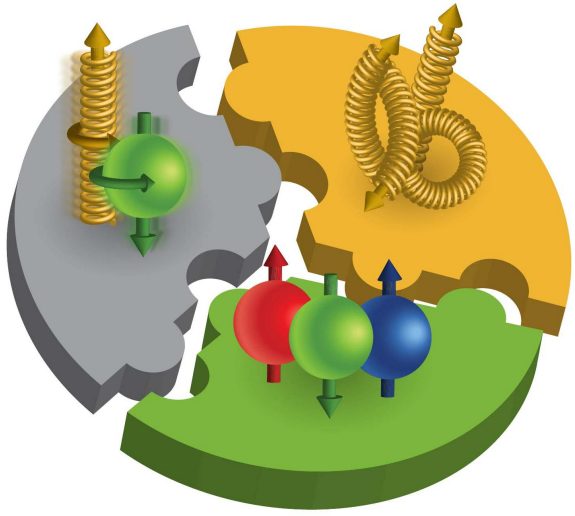

Beam-induced target depolarization at RHIC and EIC

(implications for the HJET guiding field at EIC)

Frank Rathmann

August 28, 2024

Contents

Introduction

- Development of polarized hydrogen jet (HJET) for RHIC finished 20 yrs ago.
- Many details on the technical structure and operation cannot be found in the literature, and there is also no comprehensive publication.
- Hardly anyone around to ask:
  - Tom Wise send me some unfinished paper drafts and other material.
  - I am in touch with Alexander Nass about BRP operation and most recent BRP measurement (from 2004).
- **Today's items:**
  1. Revisit **beam-induced depolarization of target atoms**
     - Bunch repetition frequency will be much larger at EIC than at RHIC
     - Goal: Understand corresponding situation at EIC
  2. **How do magnetic fields produced by beams in RHIC and EIC affect the target polarization?**
  3. **Concept for a new holding field system**

Bunch structure

RHIC situation:

- Time period between two adjacent bunches: $\tau_\mathrm{b} = \frac{\tau_\mathrm{rev}}{N_b} = 106.57\,\mathrm{ns}$
- Number of stored bunches $N_b = 120$
- Bunch frequency $f_\mathrm{b} = \frac{1}{\tau_\mathrm{b}} = 9.3831\,\mathrm{MHz}$
- Large number of harmonics contribute to induced magnetic high-frequency field close to RHIC beam, as bunches are short ($\sigma_t \approx 1.8\,\mathrm{ns}$)

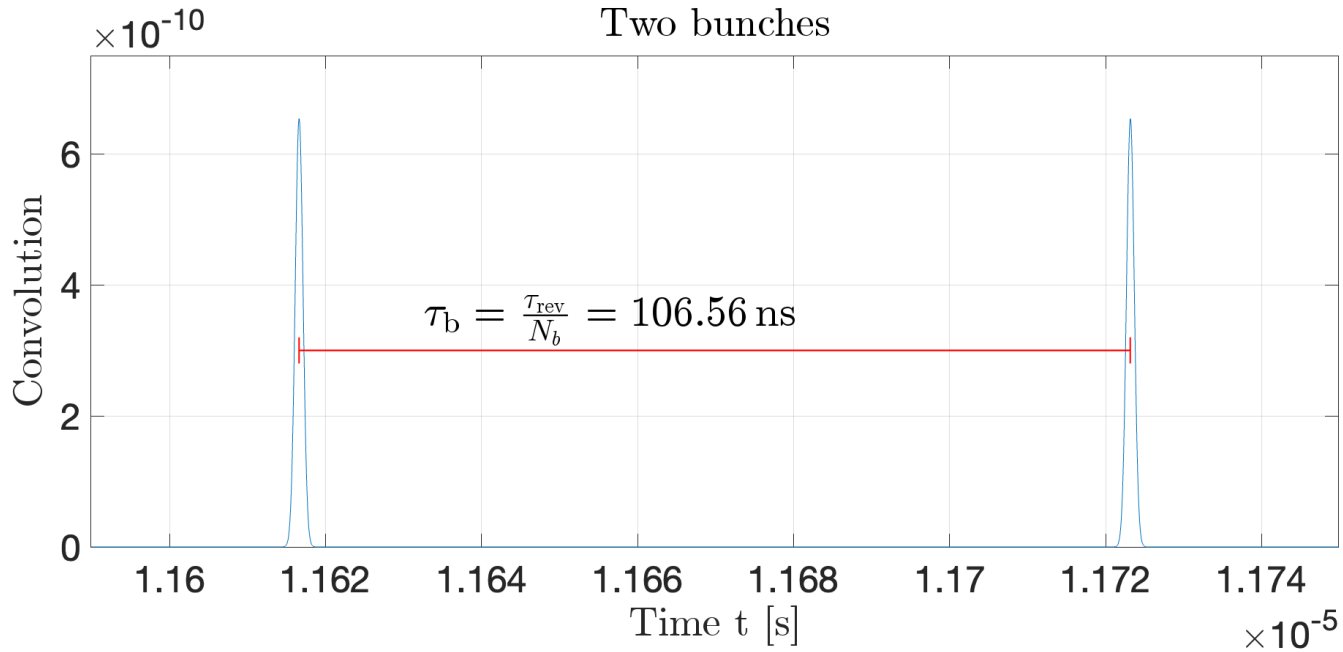

Hyperfine states of hydrogen

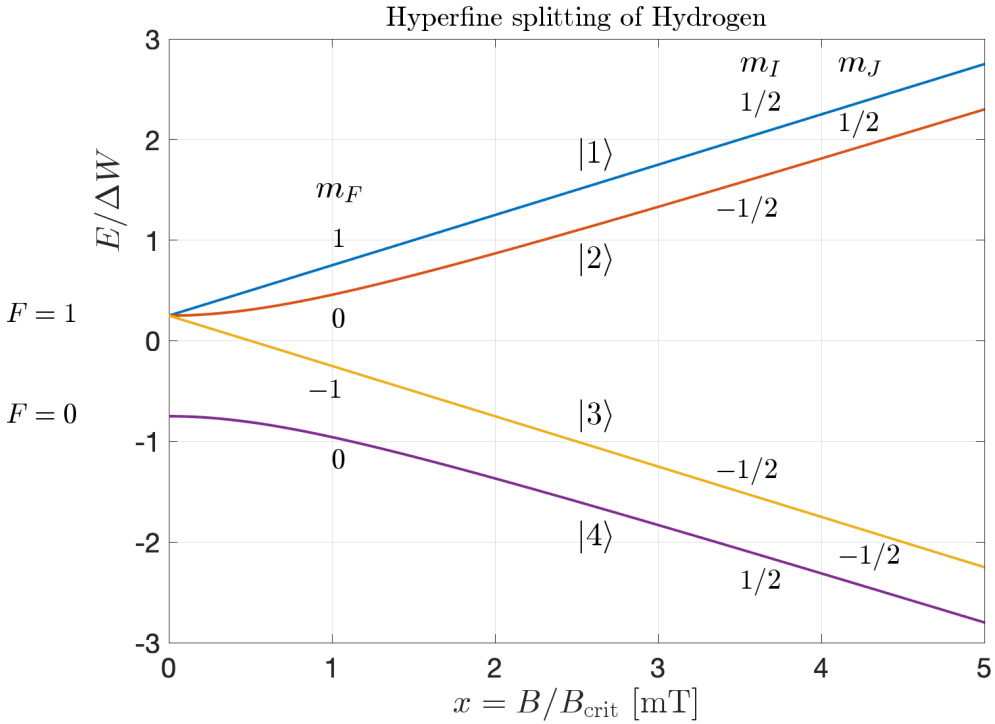

Critical field B_c (slide 47)

- Zeeman energy $g_J \mu_B B$ comparable to E_{hfs}
- $E_{\mathrm{hfs}} \approx 5.874 \times 10^{-6}$ eV ($\approx$1420 MHz [1]):
- $B_c = 50.7$ mT

Transition frequencies

- Transition frequency between two hyperfine states $|i\rangle$ and $|j\rangle$ given by:

$$f_{ij} = \frac{E_{|i\rangle}(B) - E_{|j\rangle}(B)}{h} \tag{1}$$

- When f_{ij} matches one of the beam harmonics at a certain holding field B, resonant depolarization occurs [2].

Single bunch distribution

- (Gaussian) bunch in RHIC

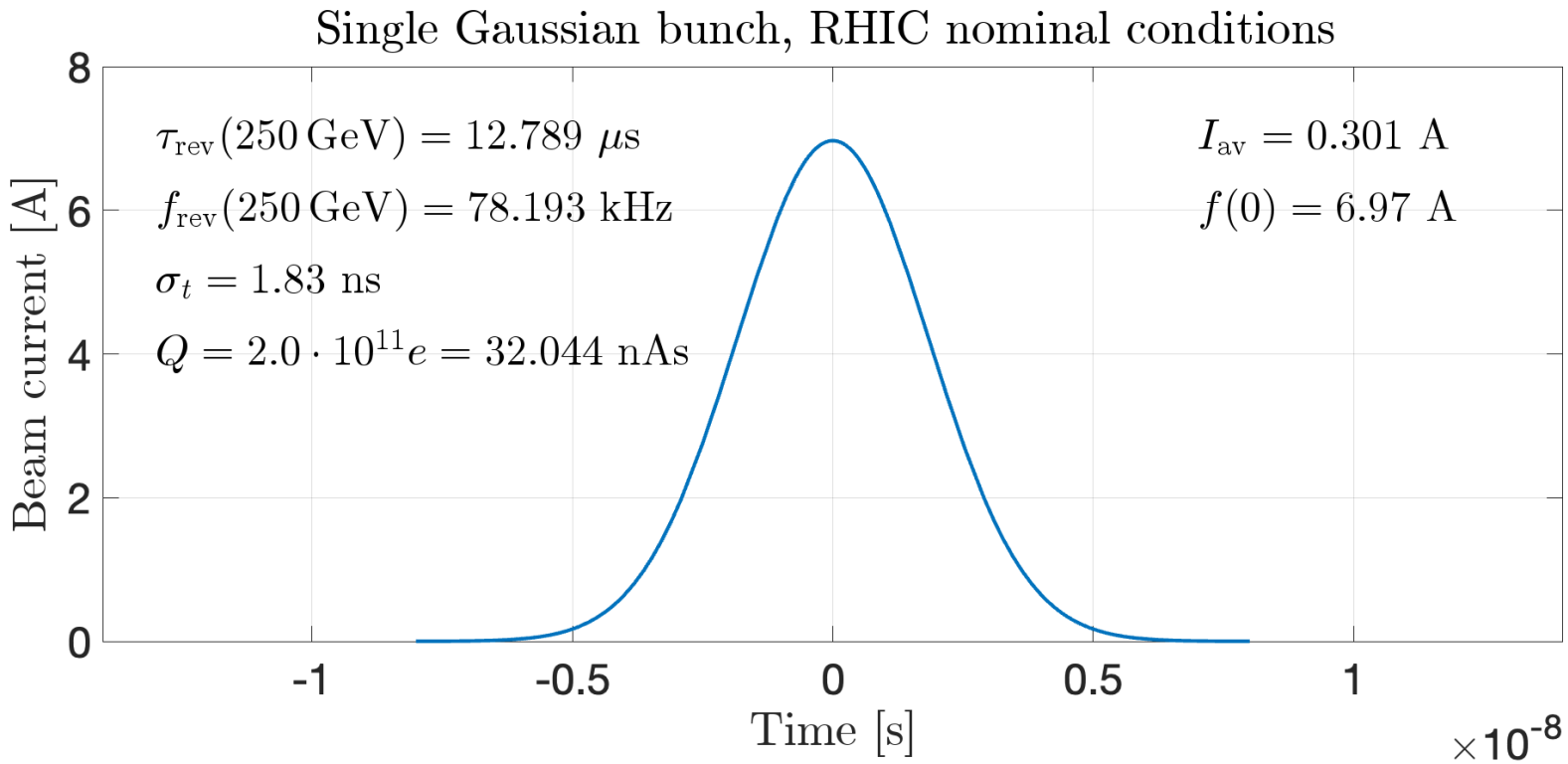

Pulse shape described by

$$f(t) = \frac{Q}{\sqrt{2\,\pi}\sigma_t} \exp\left(-\frac{t^2}{2\sigma_t^2}\right) \tag{2}$$

Gaussian convoluted with (finite) series of delta functions

Total beam current as function of time t given by

$$I(t) = \int_{-\infty}^{\infty} f(t-\xi) \sum_{k=-\infty}^{\infty} \delta\left(\xi - k\frac{\tau_{\mathrm{rev}}}{N_{\mathrm{b}}}\right) \mathrm{d}\xi \tag{3}$$

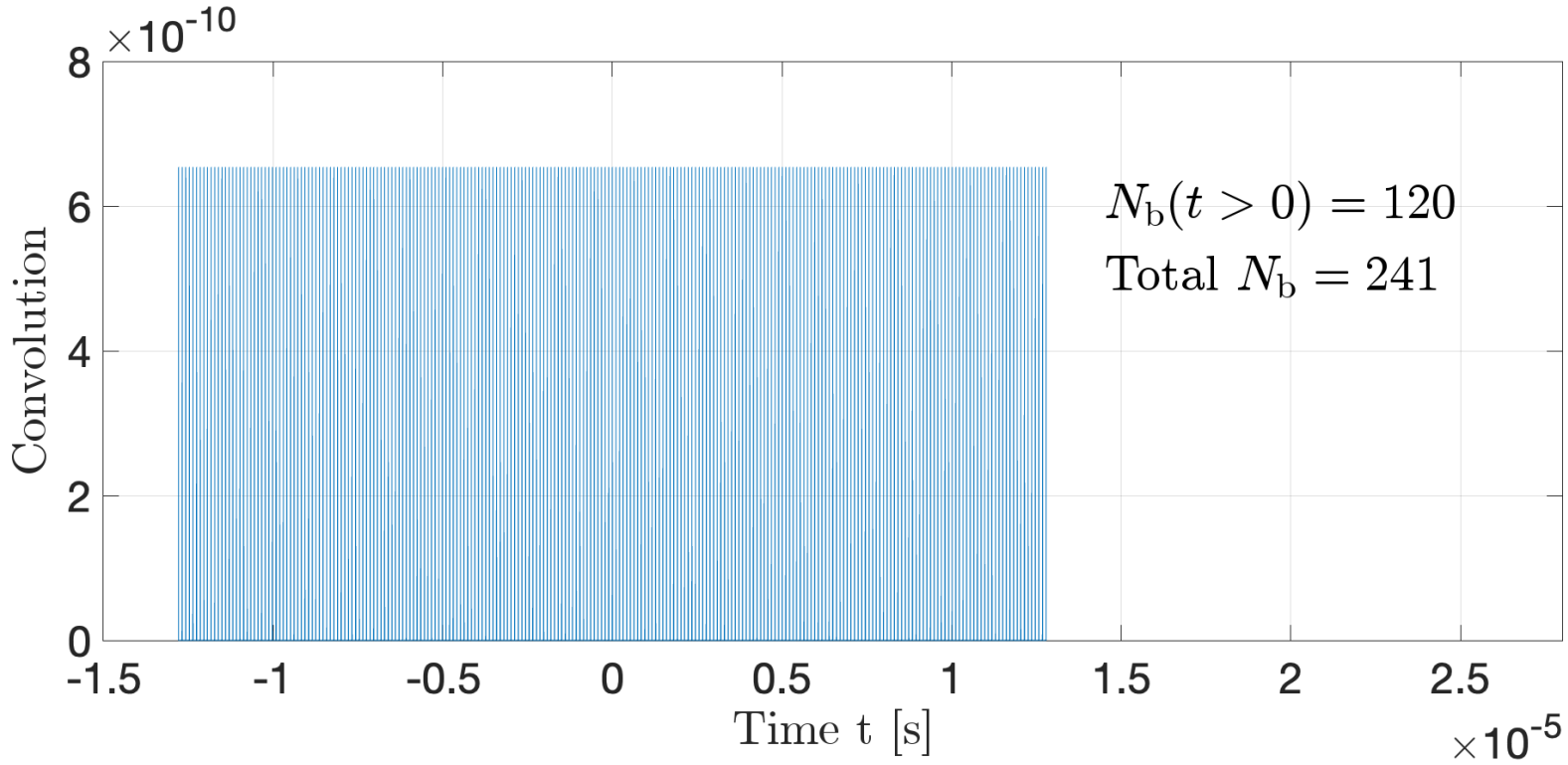

Radiofrequency-fields

FFT of convolution

- Two-sided amplitude spectrum of FFT of the convolution

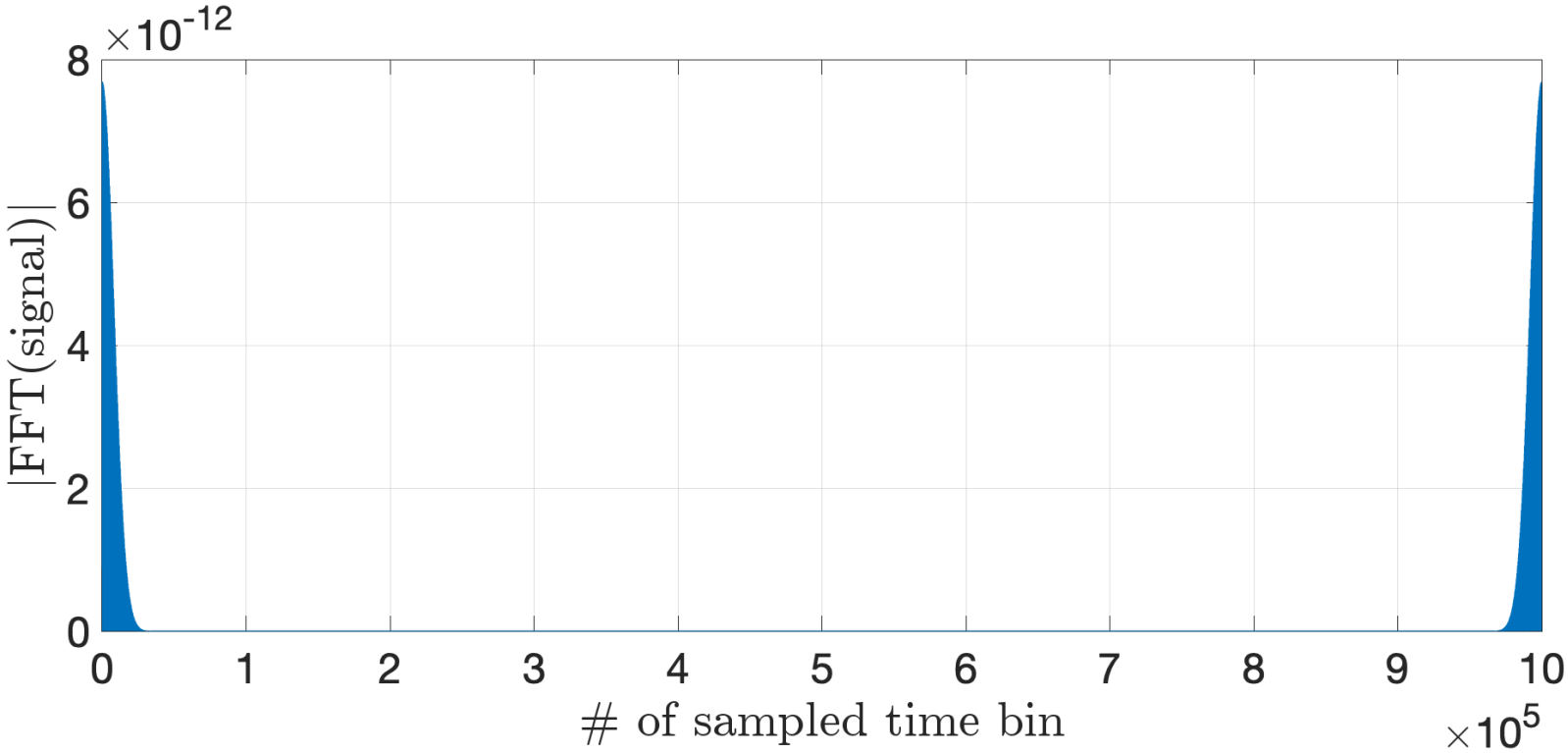

Produced radio-frequency fields

- Single-sided amplitude spectrum of FFT
- x-axis converted to frequency

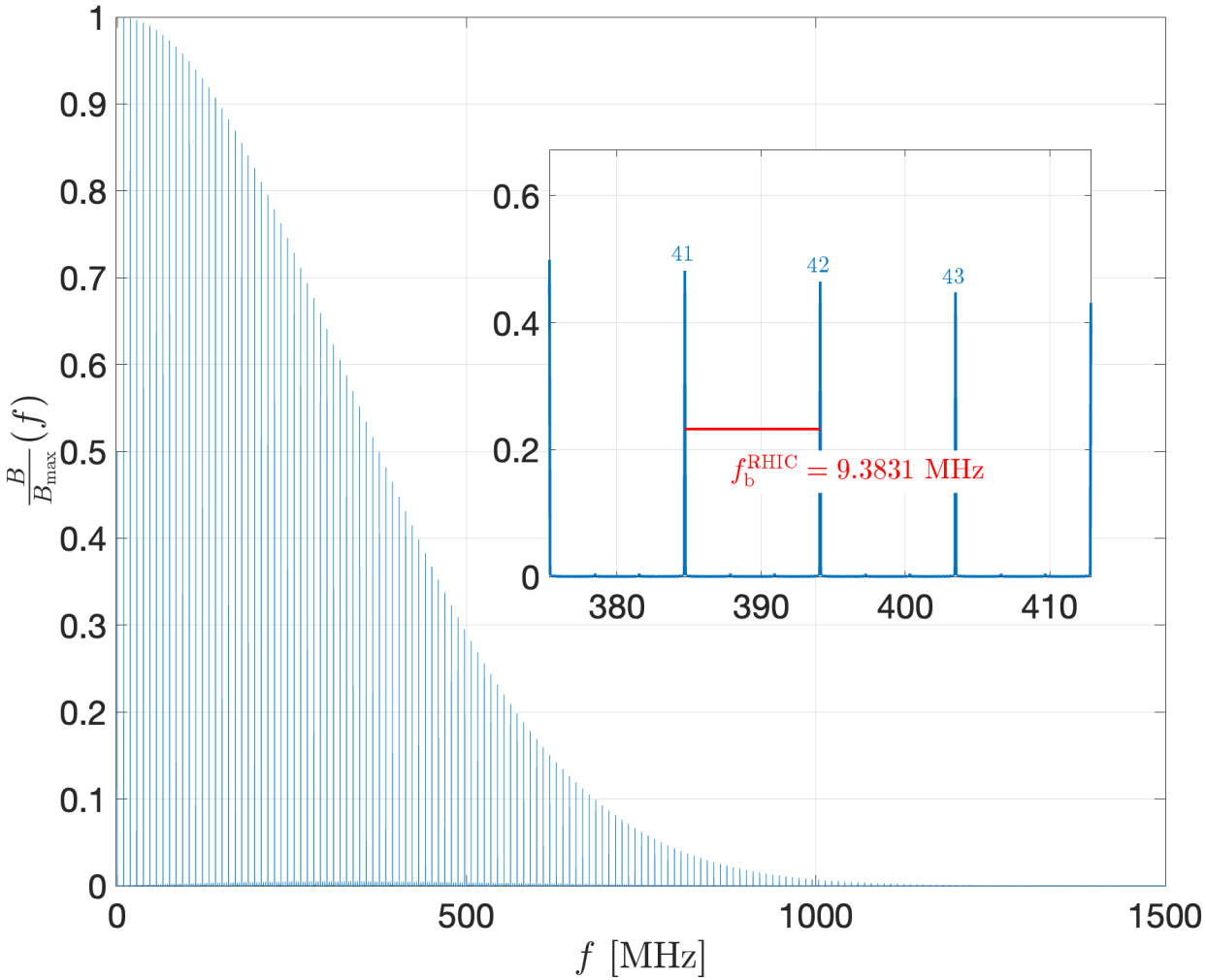

Amplitudes of magnetic RF fields

- Same, but logy
- FFT background $\leq 1\%$
  - not at f_{rev}
  - not from finite set of δ fcts
  - $\rightarrow$ probably numerical from FFT

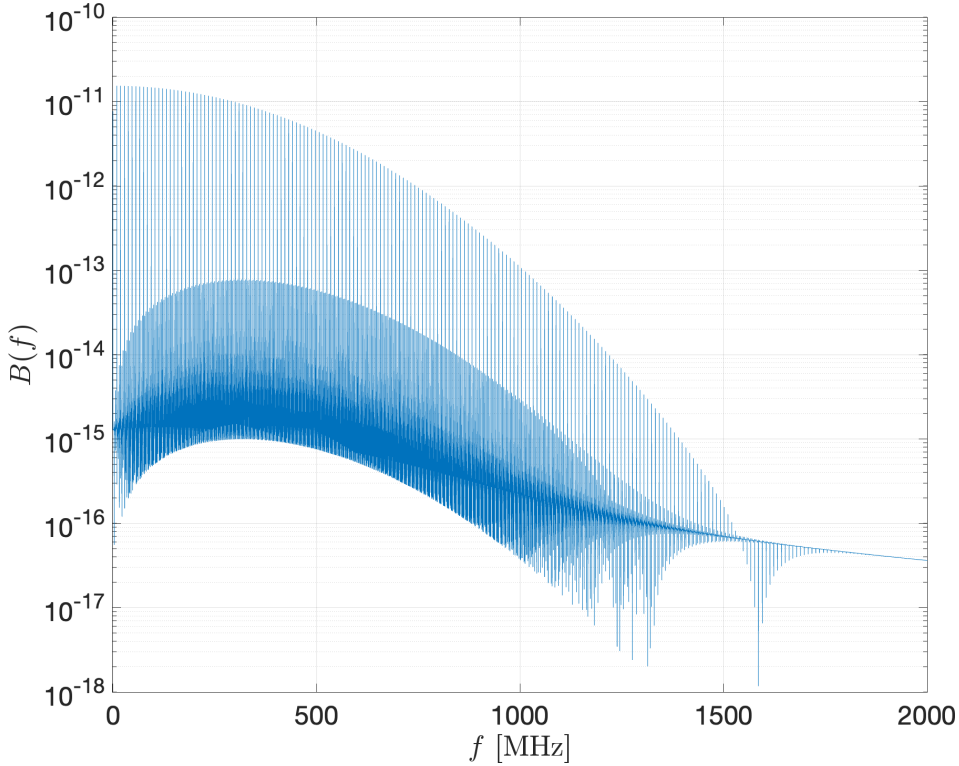

Transition frequencies between hyperfine states of H

Based on Zeeman splitting, shown on slide 5, using Eq. (1)

- Determine transition frequencies f_{ij} between hyperfine states $|i\rangle$ and $|j\rangle$.
- Cclassification refers to change of quantum numbers (see Ramsey [3]):
  - B_0 is static field, B_1 is RF field that exerts torque on magnetic moment μ:
  - π ($B_1 \perp B_0$) transitions *within one* F multiplet:

$$\Delta F = 0, \quad \Delta m_F = \pm 1. \tag{4}$$

  - σ ($B_1 \parallel B_0$) transitions *between different* F multiplets:

$$\Delta F = \pm 1, \quad \Delta m_F = 0, \pm 1. \tag{5}$$

  - Single photon transitions in H: f_{12}^{π}, f_{23}^{π}, f_{14}^{σ}, f_{24}^{σ}, and f_{34}^{σ}.
  - Transition $f_{13}^{2\gamma}$ with $\Delta m_F = 2$ requires two photons.

Transition frequencies between hyperfine states of H

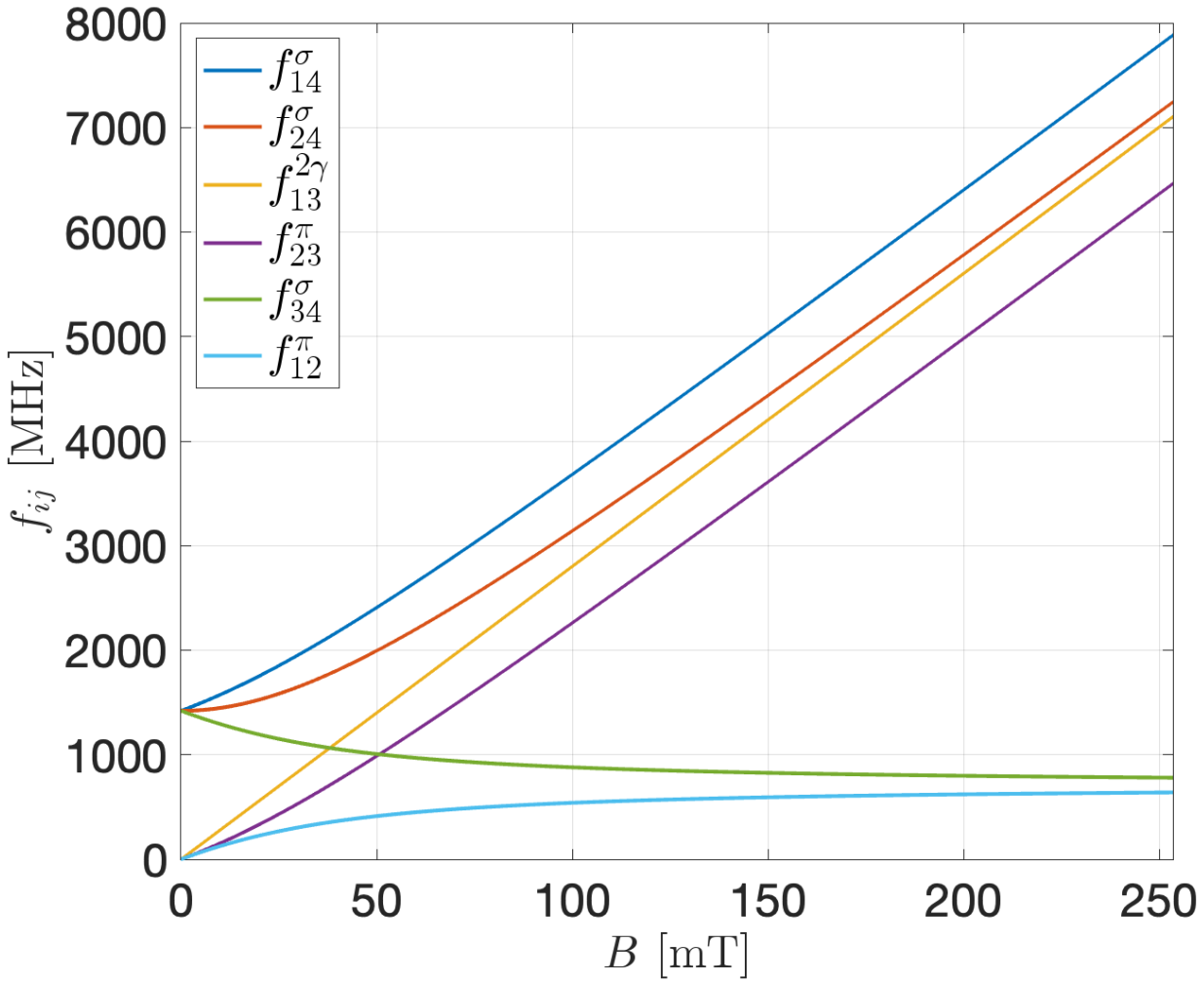

Hydrogen hyperfine transitions from bunch fields

Depolarization when f_{ij} multiple of bunch frequency f_b^{RHIC}

- HJET injects states $|1\rangle + |4\rangle$ ($p^{\uparrow}$) and $|2\rangle + |3\rangle$ ($p^{\downarrow}$).
  - What is actual orientation of B^{HJET}?

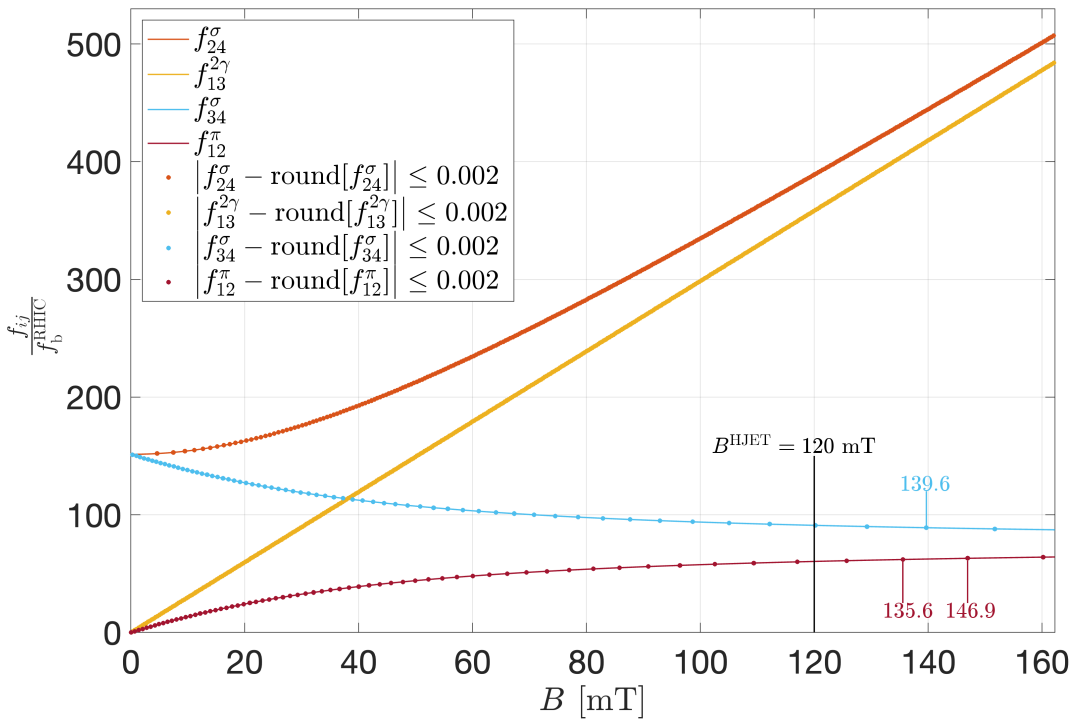

- $\left|\frac{f_{ij}}{f_b^{\mathrm{RHIC}}} - n\right| \leq 0.002\,,\ n \in \mathbb{N}$
- Same $m_I \Rightarrow f_{14}^{\sigma}$, f_{23}^{π} omitted

Single bunch distribution

- (Gaussian) bunch in EIC

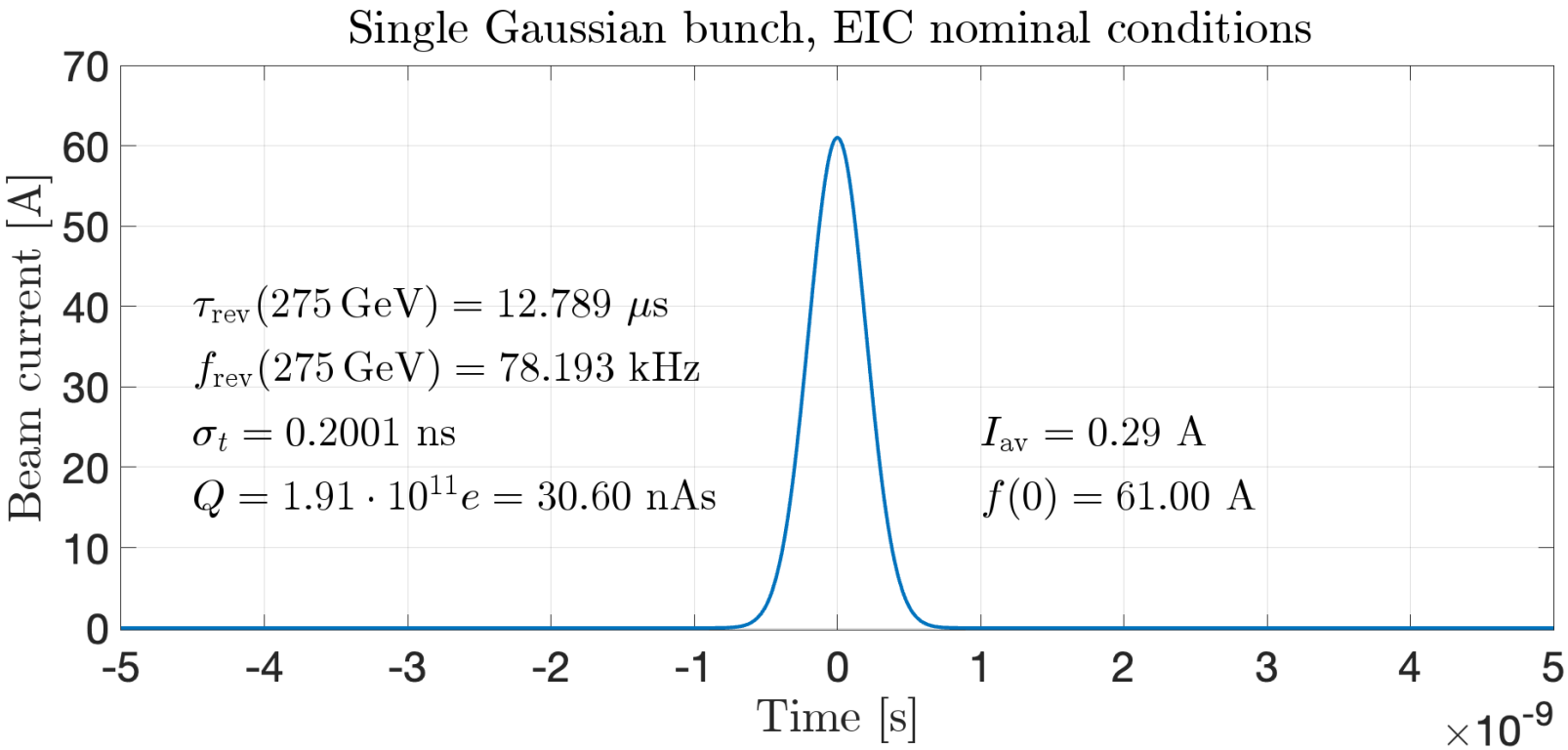

Pulse shape described by

$$f(t) = \frac{Q}{\sqrt{2\,\pi}\sigma_t} \exp\left(-\frac{t^2}{2\sigma_t^2}\right) \tag{6}$$

Bunch structure

EIC situation:

- Time period between two adjacent bunches: $\tau_\mathrm{b} = \frac{\tau_\mathrm{rev}}{N_b} = 10.85\,\mathrm{ns}$
- Number of stored bunches $N_b = 1160$
- Bunch frequency $f_\mathrm{b} = \frac{1}{\tau_\mathrm{b}} = 92.2081\,\mathrm{MHz}$

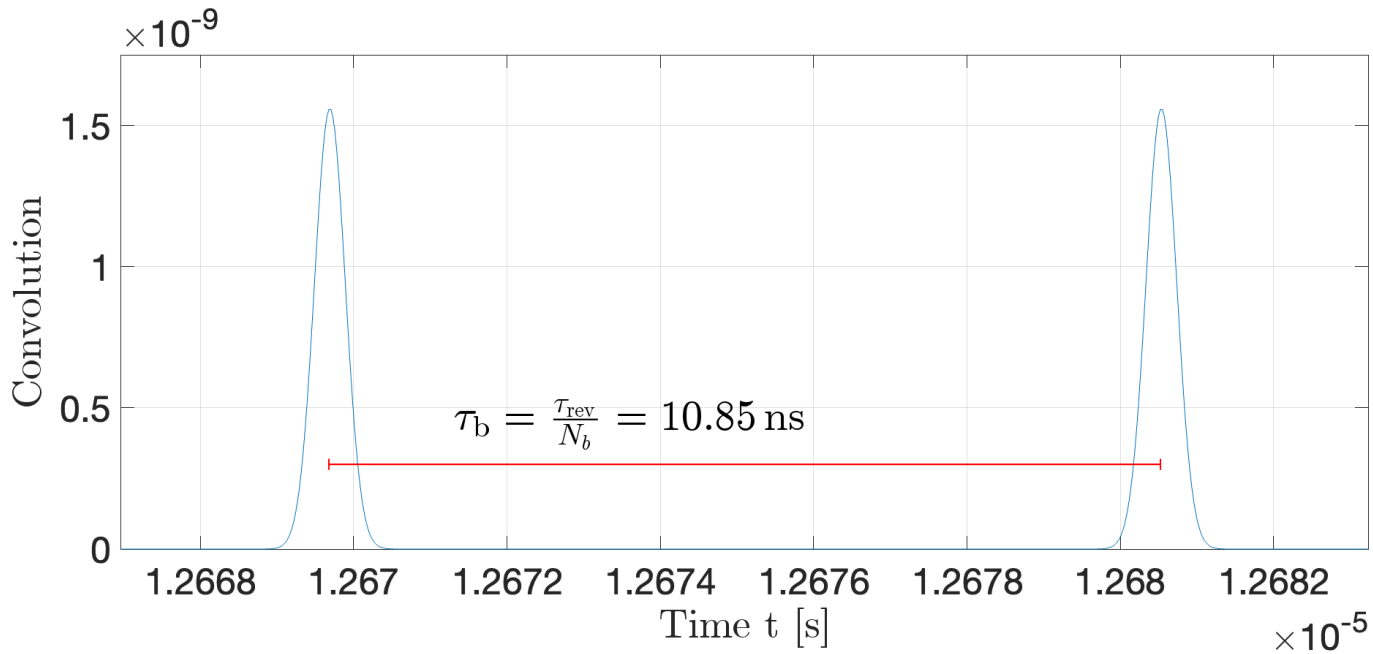

Gaussian convoluted with (finite) series of delta functions

Total beam current as function of time t given by

$$I(t) = \int_{-\infty}^{\infty} f(t-\xi) \sum_{k=-\infty}^{\infty} \delta\left(\xi - k\frac{\tau_{\mathrm{rev}}}{N_{\mathrm{b}}}\right) \mathrm{d}\xi \tag{7}$$

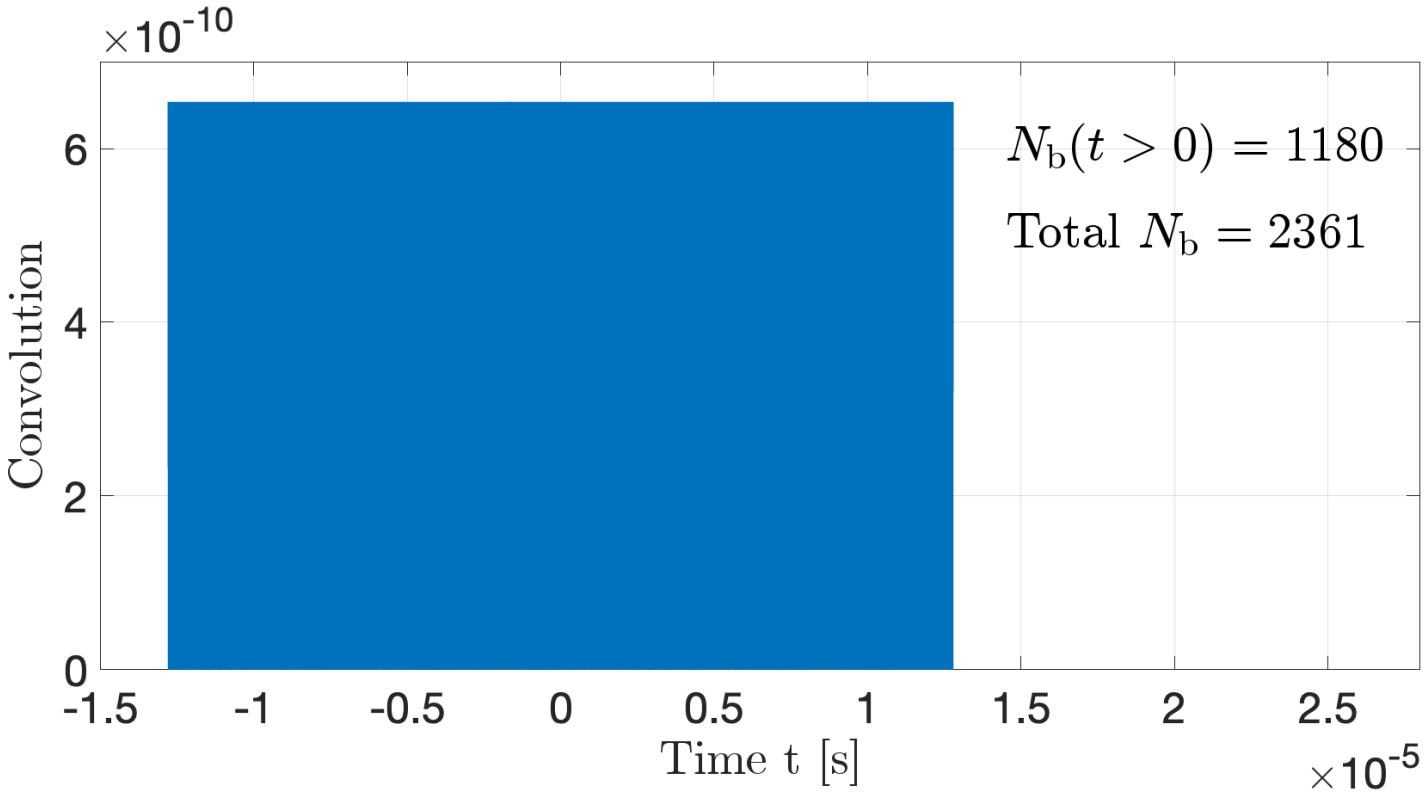

Produced radio-frequency fields

- Single-sided amplitude spectrum of FFT

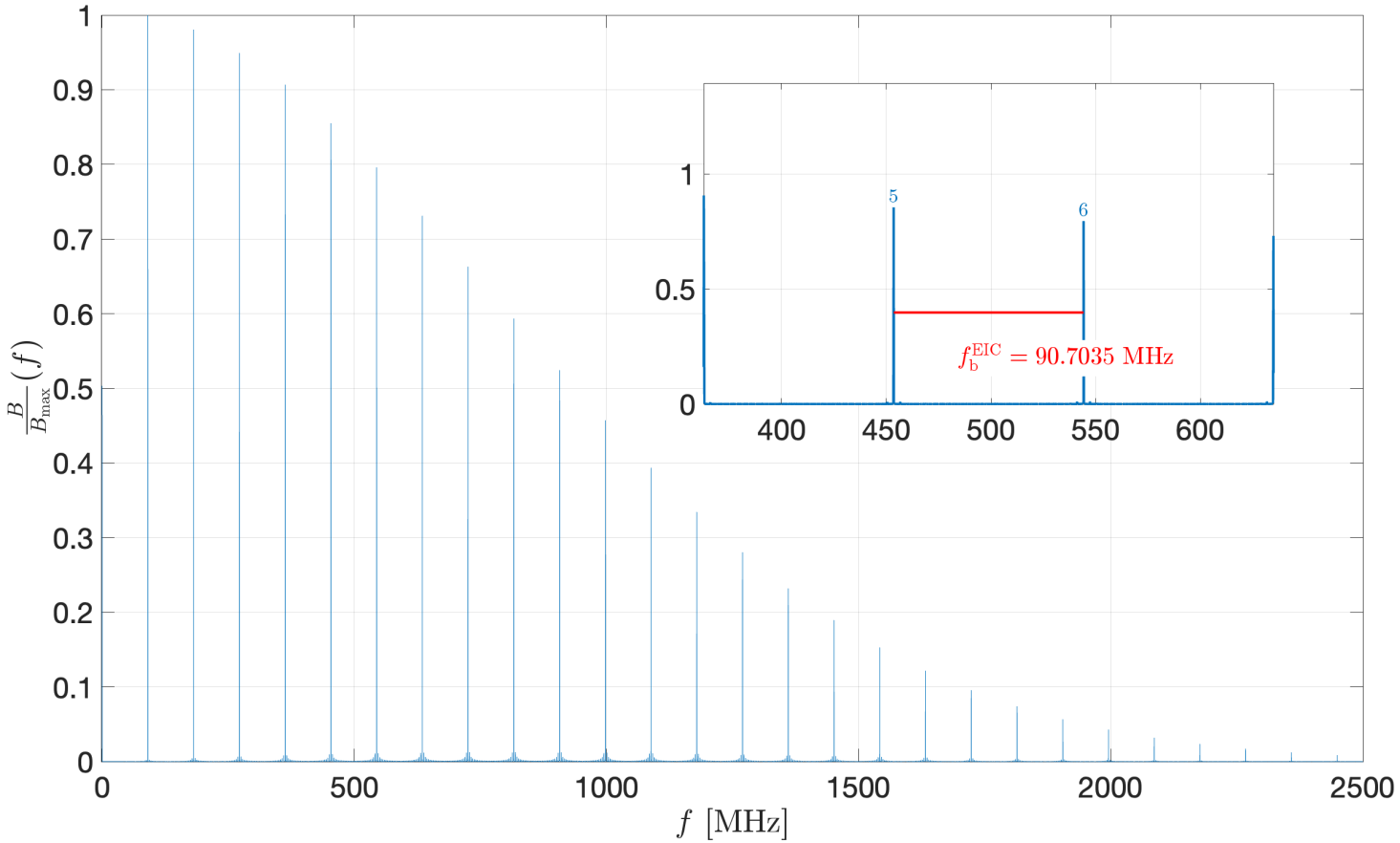

Amplitudes of radio-frequency fields

- RF field amplitudes at EIC $\approx 10\times$ larger compared to RHIC
  $\Rightarrow$ increased transition probability due more photons ($n_\gamma \propto B^2$).
- Frequency spacing in spectrum will become much larger
  $\Rightarrow$ fewer contributing resonances.

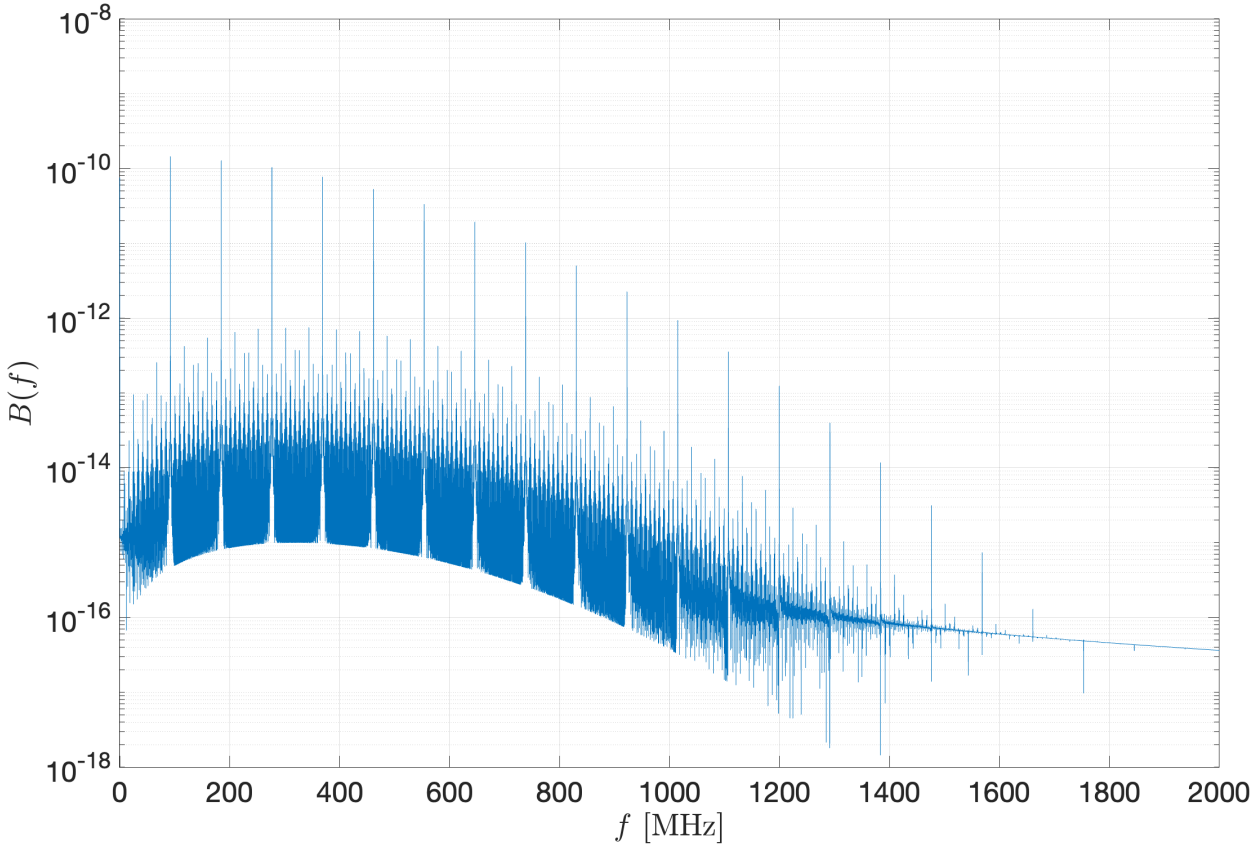

Hydrogen hyperfine transitions from bunch fields

Depolarization occurs (numerically) when $\left| \frac{f_{ij}}{f_b^{\mathrm{EIC}}} - n \right| \leq 0.002\,,\ n \in \mathbb{N}$

- For $B < 200\,\mathrm{mT}$, all transitions below harmonic number 50 will contribute!

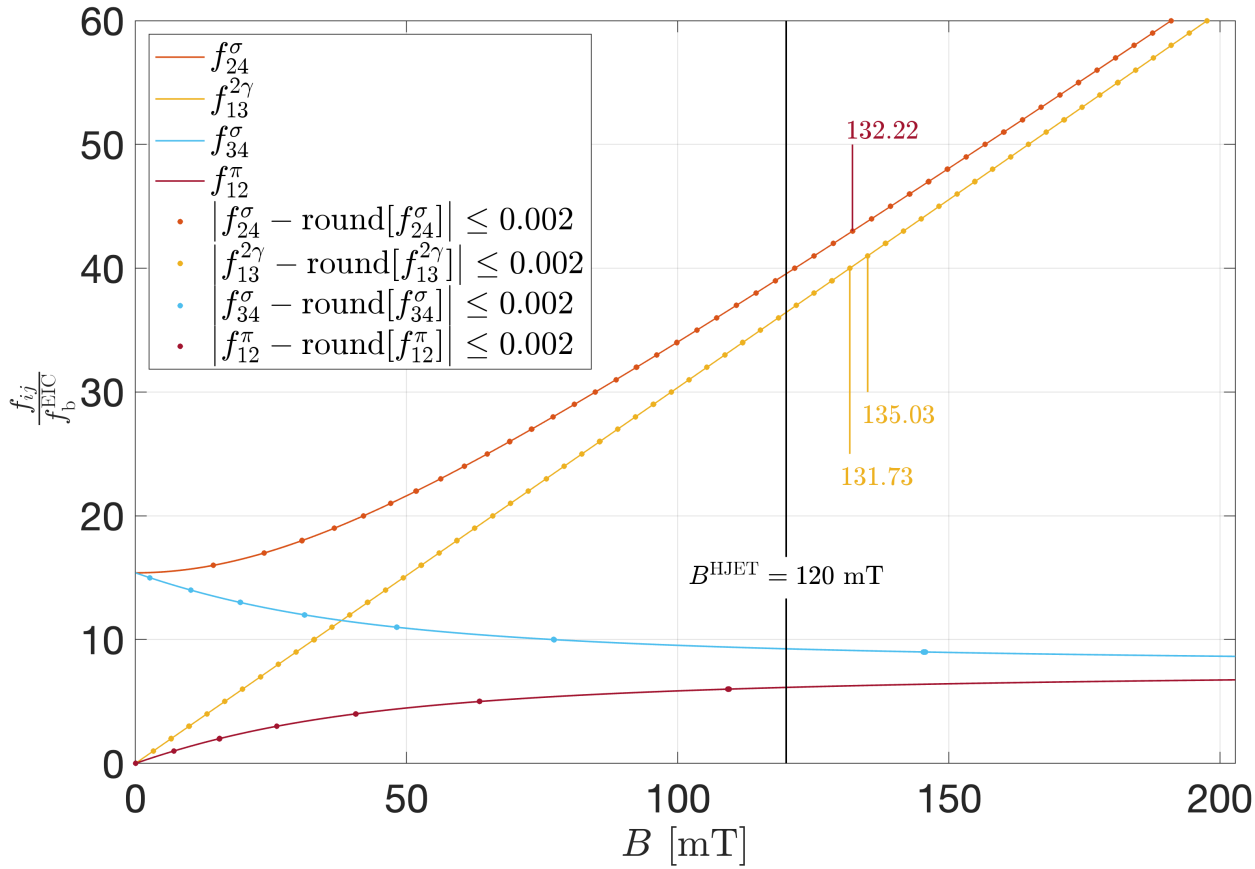

Hydrogen hyperfine transitions from bunch fields

How about the small B region?

- At RHIC, this region was inaccessible, as spacing of $f_{13}^{2\gamma} \approx 0.3\,\mathrm{mT}$.
- At EIC, at $\approx 5\,\mathrm{mT}$, spacing of $f_{13}^{2\gamma} \approx 3.3\,\mathrm{mT}$.

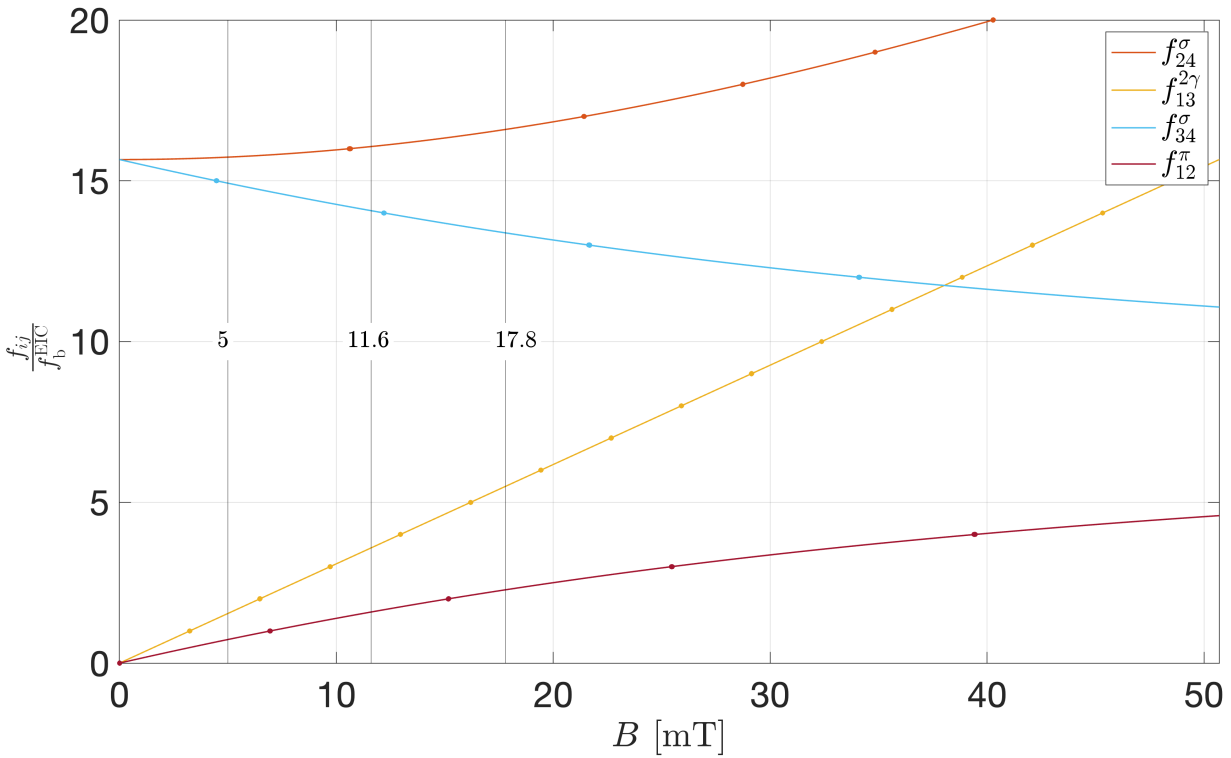

Magnetic field from beam charge

RHIC

Moving charge of beam induces magnetic field at HJET target

- β functions at the HJET in IP12 from G. Robert-Demolaize, 23.07.2024 for RHIC at top energy, determined from fill #34819,

$$\begin{aligned} \beta_x &= 8.243\,\text{m}, \beta_y = 8.326\,\text{m} \\ \beta_x &= 8.303\,\text{m}, \beta_y = 8.252\,\text{m} \end{aligned} \tag{8}$$

- Assume in the following an average $\bar{\beta}_{\text{jet}} = 8.281$
- Since $\beta_x \approx \beta_y$, we deal with a round beam. The normalized RMS emittance taken from the RHIC dashboard during run 24 is:

$$\varepsilon^N_{\text{rms}} = 2.5\,\mu\text{m}\,. \tag{9}$$

Beam parameters

RHIC

- For a Gaussian beam, assume a current density of

$$J = \frac{I(t)}{2\pi\sigma_r^2} \exp\left(-\frac{r^2}{2\sigma_r^2}\right), \quad \text{where} \quad \sigma_r = \sqrt{\frac{\bar{\beta}_{\text{jet}}\epsilon_{\text{rms}}^{\text{N}}}{k \cdot \beta\gamma}} \tag{10}$$

- Due to the symmetry of the problem, the magnetic field $\vec{B}$ will be tangential to concentric circles around the z-axis. Thus, $\vec{B}$ can be written as

$$\vec{B} = B(r)\vec{e}_\phi \tag{11}$$

- With beam traveling in $\vec{e}_z$ direction, the integration for a cylindrical Gaussian beam yields the magnetic field

$$\vec{B}(r) = \frac{\mu_0 I(t)}{2\pi r}\left[1 - \exp\left(-\frac{r^2}{2\sigma_r^2}\right)\right]\vec{e}_\phi \text{ , with } \vec{e}_\phi = \vec{e}_z \times \vec{e}_r \tag{12}$$

-

Emittance	Beam width	injection 23.5 GeV	flattop 250 GeV
$\epsilon_{\text{rms}}^N = 2.5\,\mu\text{m}$	$\sigma_r^{1\sigma} = \left(\bar{\beta}_{\text{jet}} \cdot \frac{\epsilon_{\text{rms}}^N}{\beta\gamma}\right)^{\frac{1}{2}}$	0.89 mm	0.28 mm
$\epsilon_{95}^N = \epsilon_{\text{rms}}^N \cdot 5.993$	$\sigma_r^{95} = \sigma_r^{1\sigma} \cdot \sqrt{5.993}$	2.18 mm	0.68 mm

Magnetic field from beam charge

RHIC

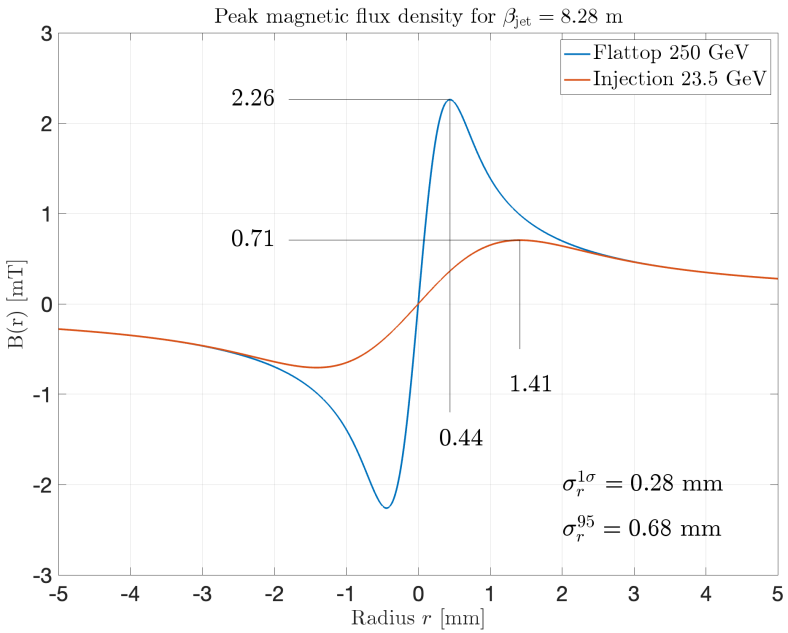

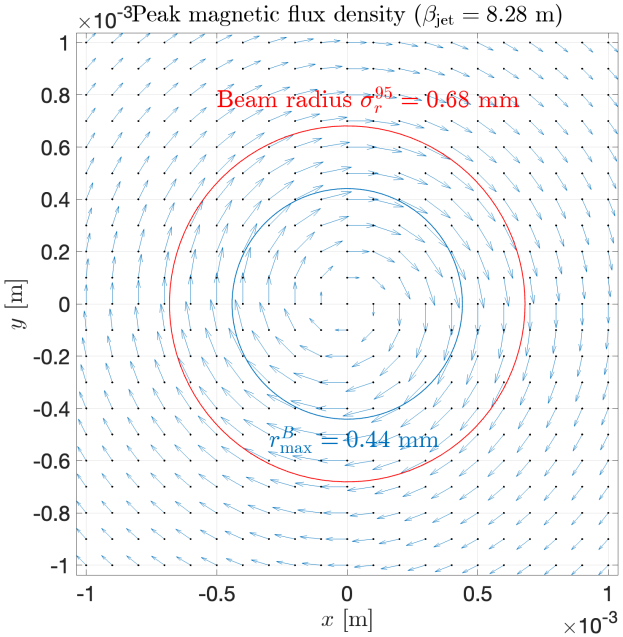

Effect on magnetic field at jet target and its polarization

RHIC

Comments for RHIC

- Systematic variation of magnetic holding field in region struck by beam:
- In the center ($r = 0$), $|\vec{B}(r)| = B_y^{\text{nom}} = 120\,\text{mT}$
- Inside the beam, magnetic fields are modified.

$$\frac{\int_0^{\sigma_r^{95}} B(r)\mathrm{d}r}{\sigma_r^{95}} = 1.73\,\text{mT} \tag{13}$$

- In the midplane ($y = 0$), still $\vec{B} \parallel \vec{e}_y$.
  - Left hemishere: $\bar{B}^{\text{L}} = 121.73\,\text{mT}$
  - Right hemishere: $\bar{B}^{\text{R}} = 118.27\,\text{mT}$

  The relative change of the target polarization inside the beam is, e.g.,

$$\delta P = \frac{P_{|1\rangle+|4\rangle}(\bar{B}^{\text{L}}) - P_{|1\rangle+|4\rangle}(\bar{B}^{\text{R}})}{P_{|1\rangle+|4\rangle}(B_y^{\text{nom}})} = 0.21\% \tag{14}$$

- In the vertical plane ($x = 0$), $\vec{B} \nparallel \vec{e}_y$.

Beam parameters

EIC

EIC beam parameters taken from Conceptual Design Report [4]

- 275 GeV
- β-functions:
  - $\beta_x = 230.323\,\text{m}$
  - $\beta_y = 69.935\,\text{m}$
  - $\rightarrow$ assumed here: $\bar{\beta} \approx 150\,\text{m}$ for future location of HJET at IP4 (from H. Lovelace, 31.07.2024).
- Like before, $\epsilon_{95}^N = \epsilon_{\text{rms}}^N \cdot 5.993$
-

beam	ϵ_{rms}^N [μm]	$\sigma_r^{1\sigma}$ [mm]	σ_r^{95} [mm]
uncooled	2.5	1.13	2.76
cooled	0.47	0.49	1.20

Magnetic field from beam charge

EIC

Uncooled beam

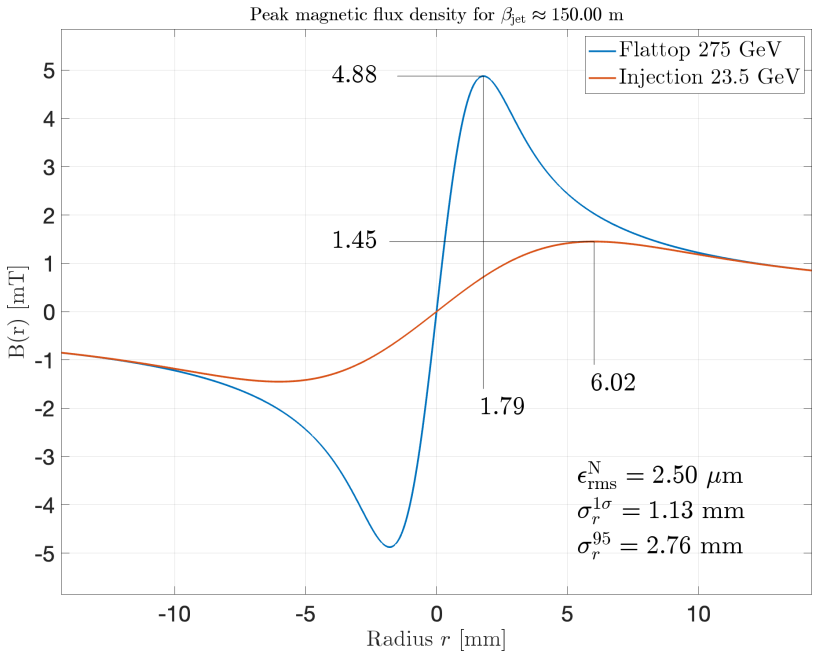

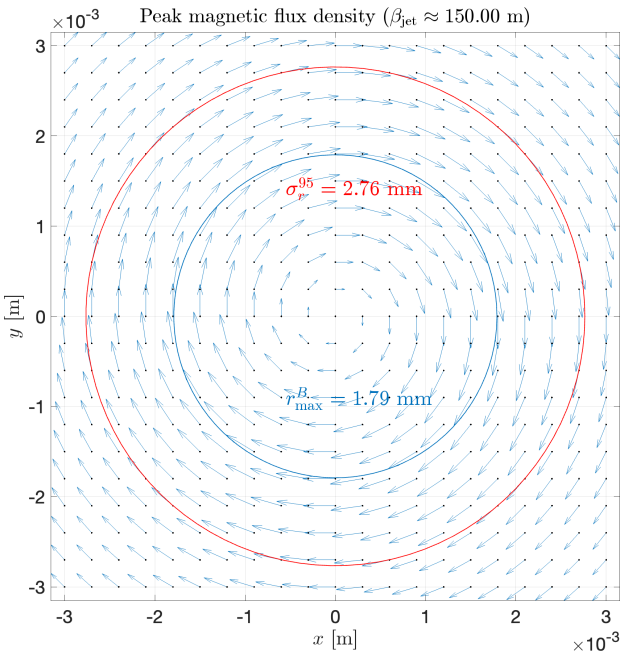

HJET beam size

- Keep in mind that on flattop, transverse dimensions of uncooled proton beam at IP4 become comparable to diameter of HJET.

Magnetic field from beam charge

EIC

Cooled beam

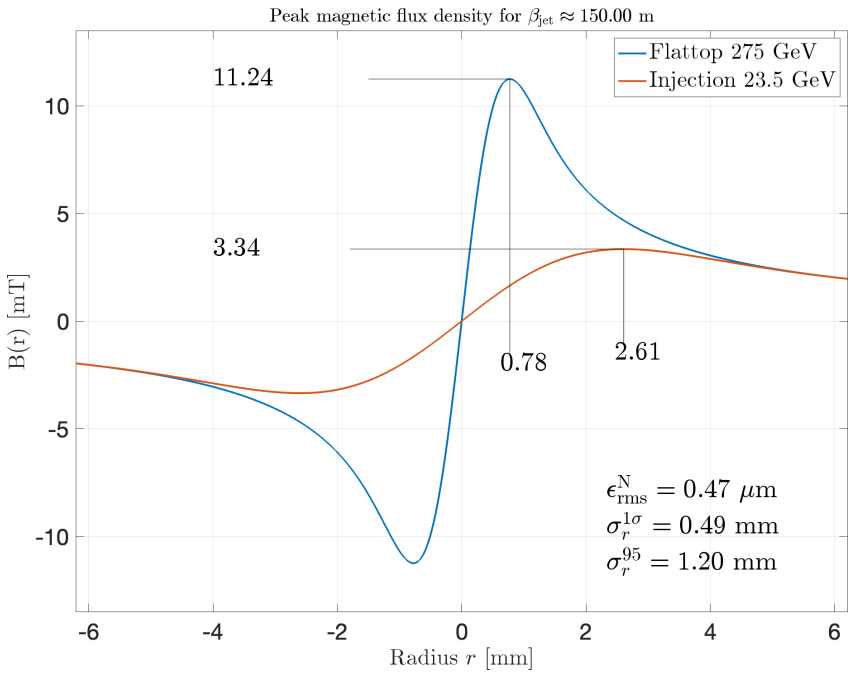

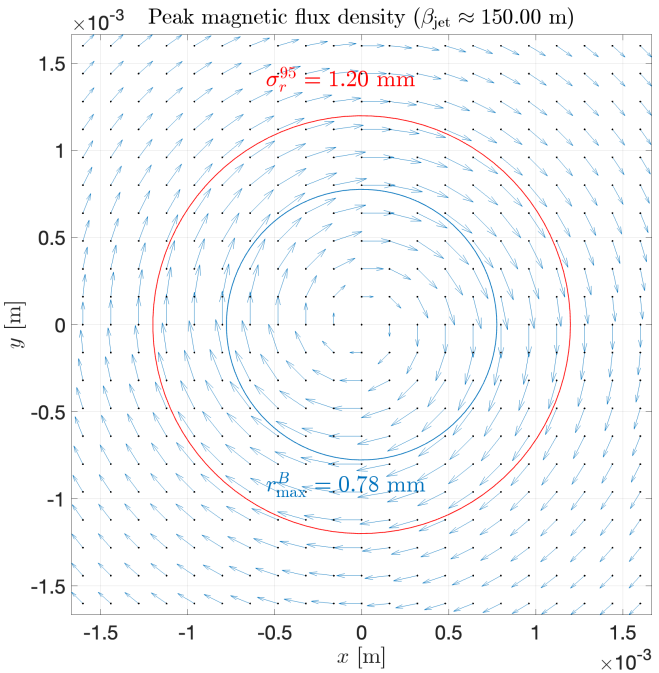

Effect on magnetic field at jet target and its polarization

EIC

Implications for EIC

1. Induced B field from beam charge:
   - uncooled beam: $B(r) \leq 4.88\,\mathrm{mT}$
   - cooled beam: $B(r) \leq 11.74\,\mathrm{mT}$

   $\rightarrow$ kills idea to apply weak holding field (20 mT) at target (slide 20)
2. Variation of polarization inside target area at 120 mT [Eq. (14)]:
   - uncooled beam: $\delta P = 0.45\%$
   - cooled beam: $\delta P = 1.05\%$
3. Variation of polarization inside target area at 350 mT [Eq. (14)]:
   - uncooled beam: $\delta P = 0.02\%$
   - cooled beam: $\delta P = 0.05\%$
4. **Due to fields induced by beam charge (item 1), beam-induced depolarizing resonances appear in HJET target** (slide 19)

Mitigation of beam-induced magnetic field effect on target

EIC

Possible solutions

1. RHIC: B-field moved to 120 mT and $\frac{f_{ij}}{f_b^{EIC}} \geq 350$ ignored (slide 13)
2. EIC: Where exactly is cutoff located for f_{24}^{σ} and $f_{13}^{2\gamma}$?
3. Strategy for EIC: $\Rightarrow$ avoid harmonics ≥ 100 $\Rightarrow$ holding field $\geq 350\,\mathrm{mT}$

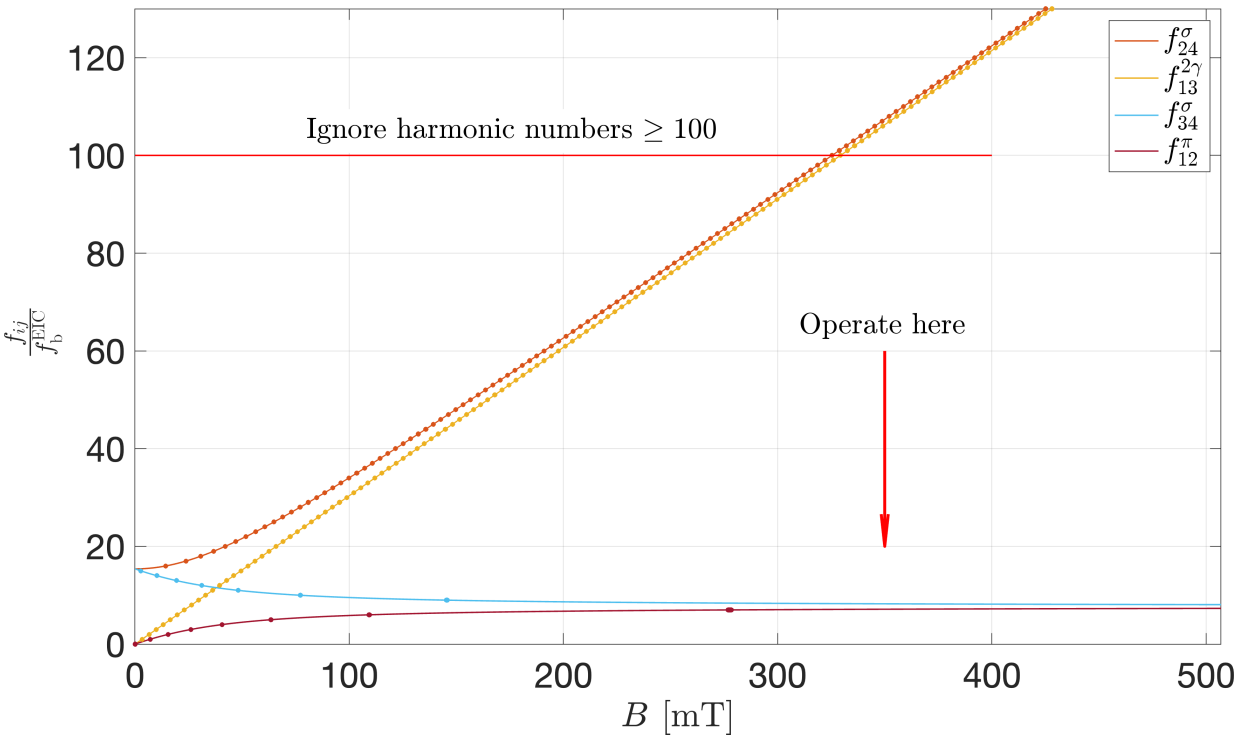

What is know from RHIC: At which B do harmonics become harmless?

Holding field system for $|\vec{B}| \approx 0.3\,\mathrm{T}$ with $\vec{B} \parallel \vec{e}_{x,y,z}$

Work together with Helmut Soltner (FZJ, Germany)

Motivation:

- Reconcile strong magnetic holding field with open detector geometry to determine all spin components of beam polarization $\vec{P} = (P_x, P_y, P_z)$
- Exploit magnetic moments $\vec{m}$ of homogeneously magnetized spheres [5–7]
- Invert $\vec{m}$ in vacuum to reverse $\vec{B}(O)$
- Reorient $\vec{m}$'s to generate $\vec{B}(O) \parallel \vec{e}_{x,y,z}$

Consider two sets of frames

- Set 1:
  - Interaction region where beam meets atoms at (O)
  - Set 1: $100\,\mathrm{mm}_x \times 100\,\mathrm{mm}_y \times 40\,\mathrm{mm}_z$ and
    Set 2: $100\,\mathrm{mm}_x \times 100\,\mathrm{mm}_y \times 110\,\mathrm{mm}_z$, centered around x, y, and z axes.
  - 8 permanently magnetized spheres in each corner of each frame:
    - NeFeB magnets provide remanence of $B_r = 1.49 - 1.55\,\mathrm{T}$ (type N58)
    - Radius $r = 30\,\mathrm{mm}$

Holding field system for $|\vec{B}| \approx 0.3\,\mathrm{T}$ with $\vec{B} \parallel \vec{e}_{x,y,z}$

Together with Helmut Soltner (FZJ, Germany)

Calculation

- Flux density vector as function of $\vec{m}$ in space

$$\vec{B}(\vec{r}) = \frac{\mu_0}{4\pi}\left[\frac{3\left(\vec{m}\cdot\hat{R}\right)\hat{R} - \vec{m}}{|R|^3}\right], \tag{15}$$

where $\vec{R} = \vec{r} - \vec{r}_0$, $\hat{R} = \frac{\vec{R}}{|R|}$.

- Optimize orientation of $\vec{m}$'s to maximize $\vec{B}(O)$ in x, y, and z direction:
  - maximize dot product $\vec{m}\cdot\hat{R}$ and set $m_y = 0$, to obtain, e.g., max. B_y.

Component $B_x(O)$ using two sets of $\vec{m}$'s

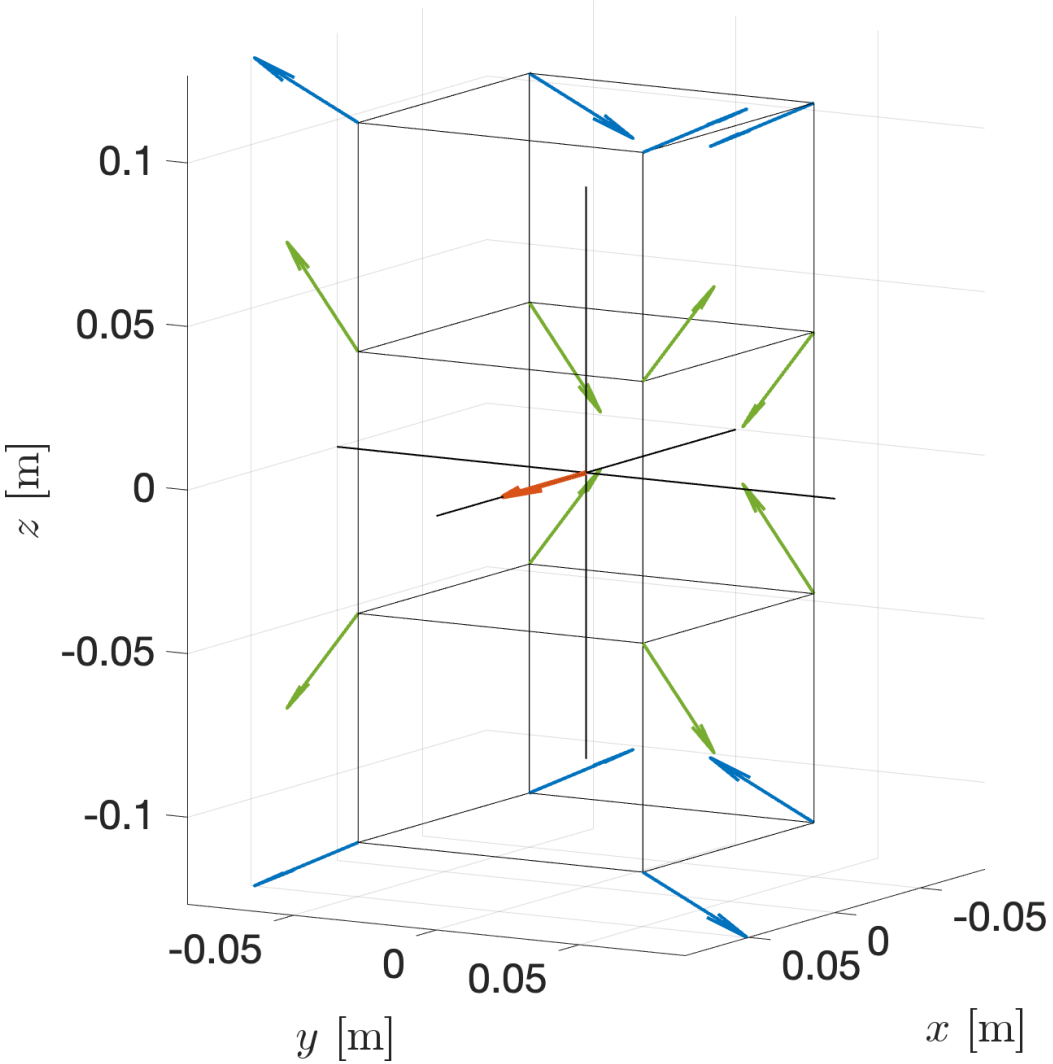

$$B_x: \begin{pmatrix} 0.3224 \\ 0 \\ 0 \end{pmatrix} \mathrm{T}$$

Component $B_y(O)$ using two sets of $\vec{m}$'s

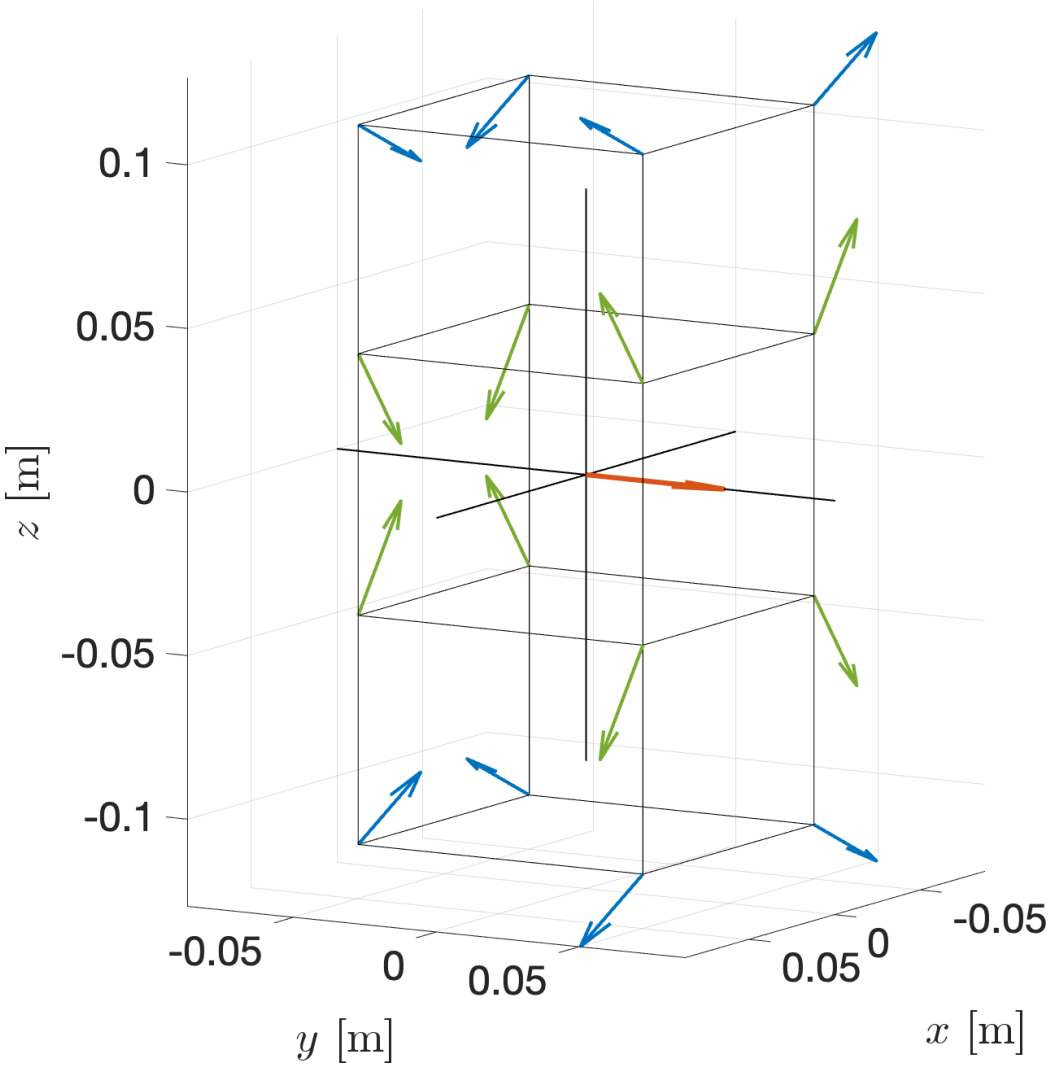

$$B_y: \begin{pmatrix} 0 \\ 0.3224 \\ 0 \end{pmatrix} \mathrm{T},$$

Component $B_z(O)$ using two sets of $\vec{m}$'s

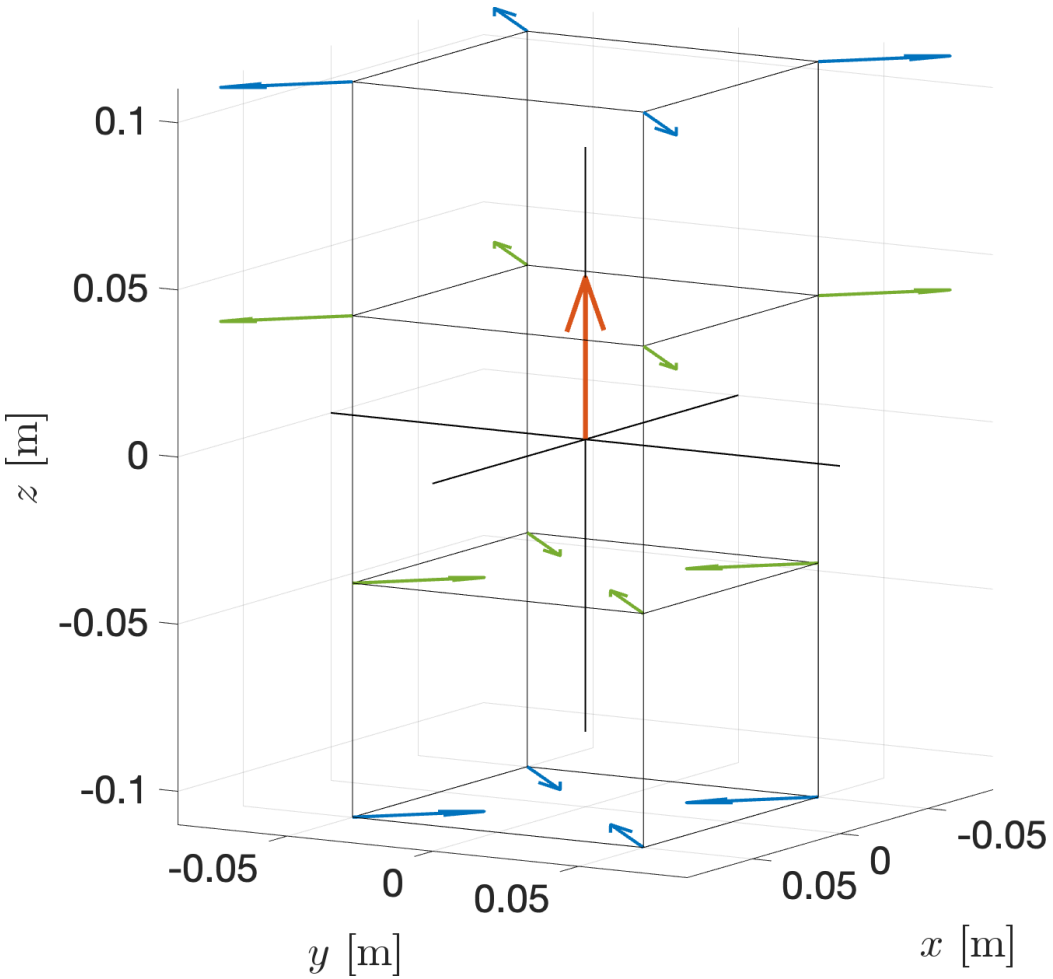

$$B_z: \begin{pmatrix} 0 \\ 0 \\ 0.3227 \end{pmatrix} \mathrm{T}$$

Technical realization

With properly rotated spheres

- Setup allows for azimuthally symmetric detector setup with acceptance $\Delta\phi \approx \pm 15^\circ$ at $\phi = 45$, 135, 225, and 315°
  - $\phi = \arctan(30/50) = 31^\circ$
- Technically challenging will be:
  1. Accurate reorientation of magnetized spheres in vacuum
  2. Vacuum compatible coatings, like Ni, or stainless steel covers to prevent Hand H_2 to deteriorate NeFeB

Force and torque between two dipoles $\vec{m}_1$ and $\vec{m}_2$ I

Potential energy of magnetic dipole

$$U = -\vec{m} \cdot \vec{B}$$
$$\vec{F} = -\vec{\nabla} U \quad \rightarrow \quad F_{12} = \vec{\nabla}\left(\vec{m}_2 \cdot \vec{B}_1\right) \tag{16}$$

- $\vec{B}_1$ is flux density produced by $\vec{m}_1$ at location of $\vec{m}_2$.

Force:

$$\vec{F}_{12}(\vec{r}_{12}, \vec{m}_1, \vec{m}_2) = \frac{3\mu_0}{4\pi r_{12}^4}\Big[\vec{m}_2\left(\vec{m}_1 \cdot \vec{e}_{12}\right) + \vec{m}_1\left(\vec{m}_2 \cdot \vec{e}_{12}\right) + \vec{e}_{12}\left(\vec{m}_1 \cdot \vec{m}_2\right) - 5\vec{e}_{12}\left(\vec{m}_1 \cdot \vec{e}_{12}\right)\left(\vec{m}_2 \cdot \vec{e}_{12}\right)\Big] \tag{17}$$

- $\vec{r}_{12}$ is vector between $\vec{m}_1$ and $\vec{m}_2$, $\vec{e}_{12} = \frac{\vec{r}_{12}}{|r_{12}|}$.

Torque

$$\vec{\tau} = \vec{m}_2 \times \vec{B}_1 \tag{18}$$

Force and torque between two dipoles $\vec{m}_1$ and $\vec{m}_2$ II

Examples: $\vec{m}_1 \perp \vec{m}_2$

1. Spheres touch:

$$r_{12} = 0.06\,\mathrm{m} \quad \vec{F}_{12} = -417\,\mathrm{N} \quad \tau_{12} = 8.3\,\mathrm{Nm} \tag{19}$$

2. System assembled:

$$r_{12} \geq 0.07\,\mathrm{m} \quad \vec{F}_{12} \leq -225\,\mathrm{N} \quad \tau_{12} = 5.2\,\mathrm{Nm} \tag{20}$$

Flux density of system in 3D

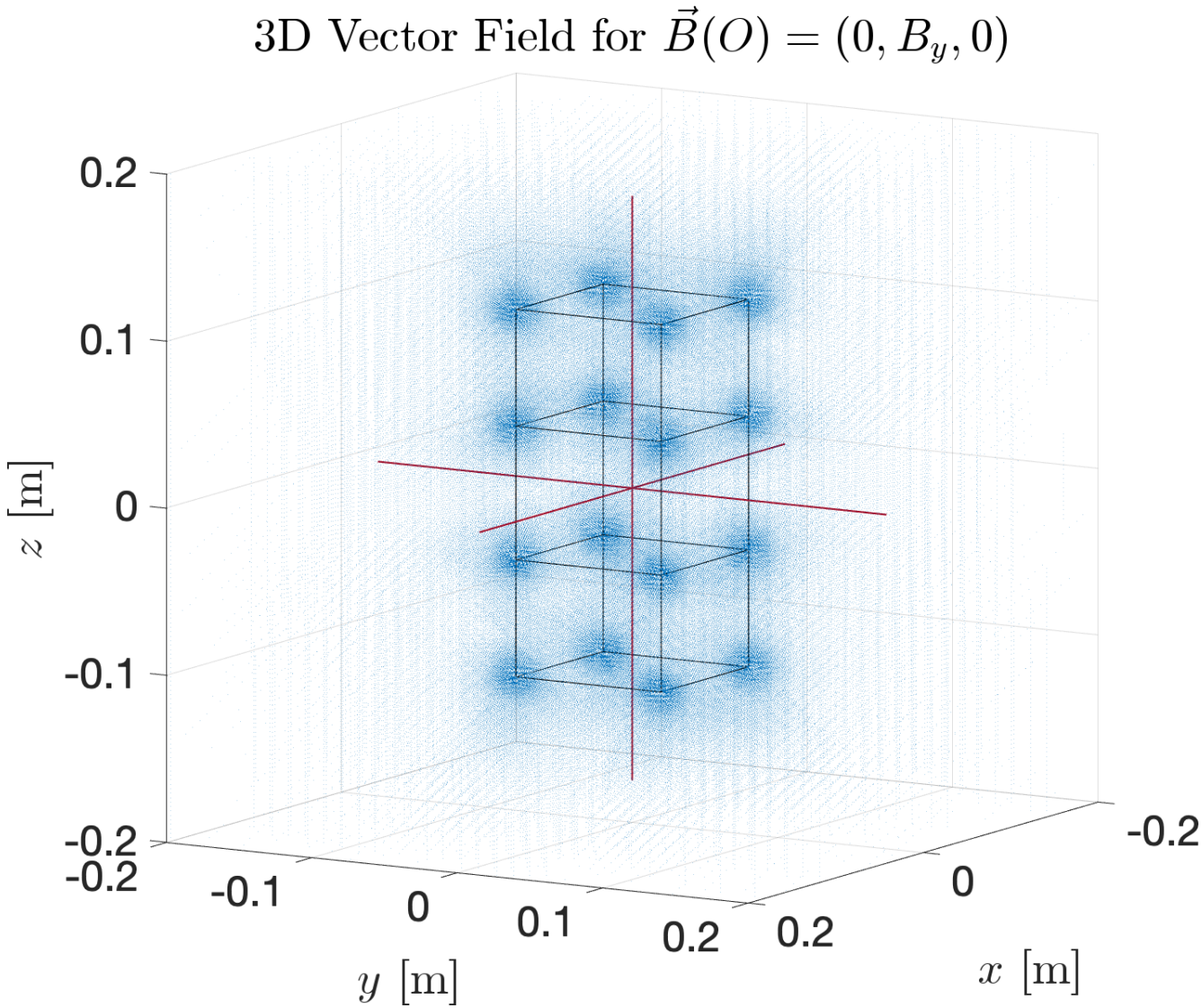

Check assembly for zero crossings along the axes

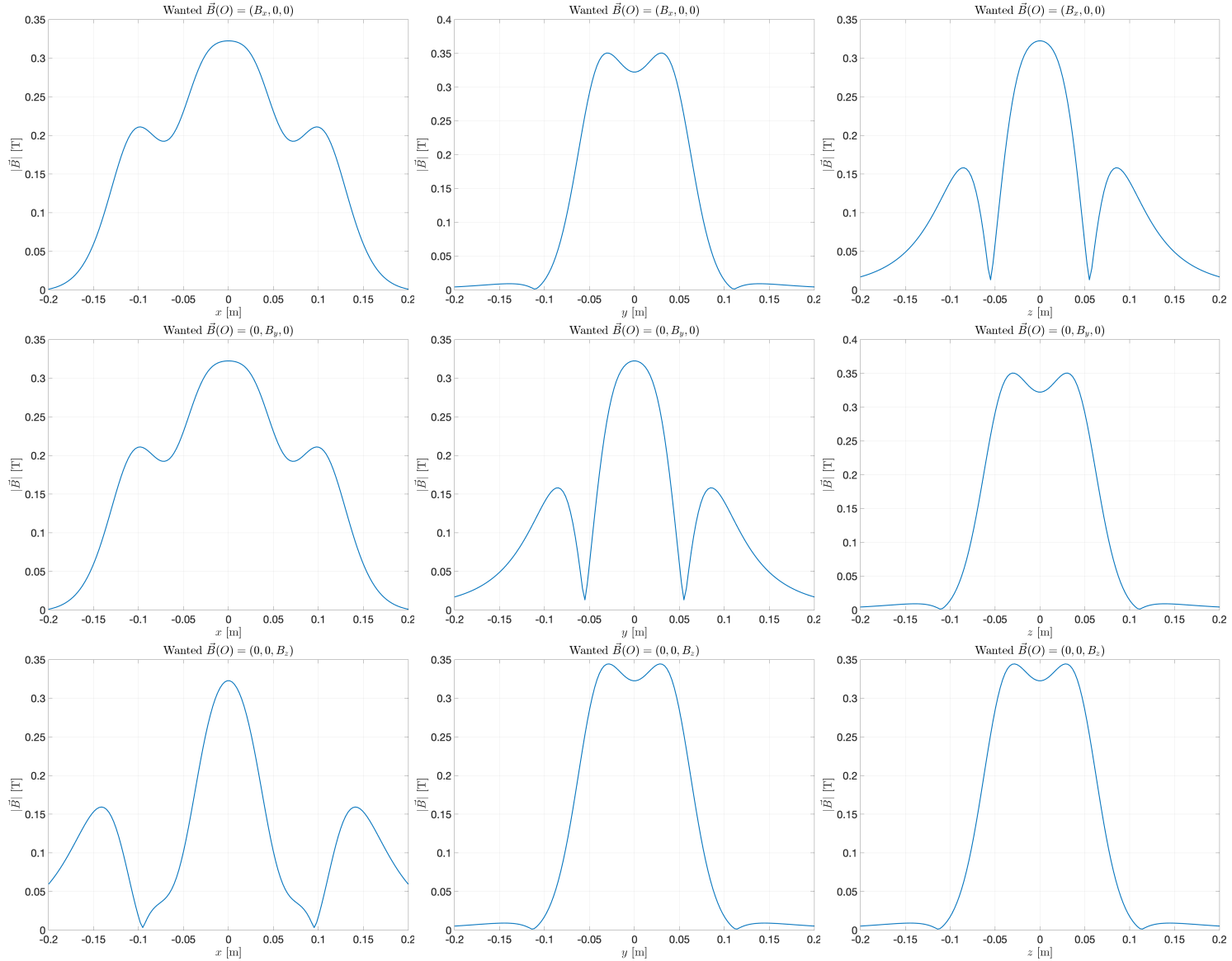

Conclusion

Conclusion

1. Bunch-induced depolarization in H target
   - RHIC: harmonic numbers > 350 were ignored.
   - EIC: All depolarizing transitions appear at harmonic numbers < 50.
2. Beam-induced magnetic fields perturb target polarization
   - RHIC: Magnetic field involved: $B(r) \leq 2.3\,\mathrm{mT}$
   - EIC: uncooled $B(r) < 4.9\,\mathrm{mT}$
   - EIC: cooled $B(r) < 11.7\,\mathrm{mT}$
3. Holding field of $|\vec{B}| \geq 300\,\mathrm{mT}$ avoids beam-induced depolarization
   - Concept using permanent magnets (NdFeB) appears feasible
   - Allows for orientation of holding field $\vec{B}$ in any direction (along x, y, or z)
   - System will allow to provide holding field $\vec{B} = 0$
   - No zero crossings along ABS axis present, $|\vec{B}(0, y, 0)| \gtrsim 1\,\mathrm{mT}$
   - May need compensation to make $\int B_{x,y} \mathrm{d}\ell = 0$ along beam direction
4. D and ^{3}He atoms:
   - Study bunch-induced depolarization
   - Study beam-induced $\vec{B}$ field effects on target polarizations

Outlook

Other things that need to be looked into

1. Zero-crossings along the vertical axis of present HJET.
   - Revisit magnetic field calculations of HJET holding field $\rightarrow$ in progress.
2. Polarization measurements with all transition units in ABS and BRP.
3. Tracking of atoms in HJET & sextupole magnet systems
   - Recuperated tracking code used originally for HJET design from Michelle/Paolo $\rightarrow$ will be time consuming to make it work

References I

[1] M. Diermaier, C. B. Jepsen, B. Kolbinger, C. Malbrunot, O. Massiczek, C. Sauerzopf, M. C. Simon, J. Zmeskal, and E. Widmann, "In-beam measurement of the hydrogen hyperfine splitting and prospects for antihydrogen spectroscopy," *Nature Commun.*, vol. 8, p. 5749, 2017, 1610.06392.

[2] A. Airapetian, N. Akopov, Z. Akopov, M. Amarian, A. Andrus, E. Aschenauer, W. Augustyniak, R. Avakian, A. Avetissian, E. Avetissian, P. Bailey, D. Balin, C. Baumgarten, M. Beckmann, S. Belostotski, N. Bianchi, H. Blok, H. Böttcher, A. Borissov, A. Borysenko, M. Bouwhuis, B. Braun, A. Brüll, V. Bryzgalov, G. Capitani, M. Capiluppi, T. Chen, G. Ciullo, M. Contalbrigo, G. Court, P. Dalpiaz, R. De Leo, M. Demey, L. De Nardo, E. De Sanctis, E. Devitsin, P. Di Nezza, M. Düren, M. Ehrenfried, A. Elalaoui-Moulay, G. Elbakian, F. Ellinghaus, U. Elschenbroich, R. Fabbri, A. Fantoni, A. Fechtchenko, L. Felawka, S. Frullani, G. Gapienko, V. Gapienko, F. Garibaldi, K. Garrow, G. Gavrilov, V. Gharibyan, G. Graw, O. Grebeniouk, I. Gregor, C. Hadjidakis, W. Haeberli, K. Hafidi, M. Hartig, D. Hasch, D. Heesbeen, M. Henoch, R. Hertenberger, W. Hesselink, A. Hillenbrand, M. Hoek, Y. Holler, B. Hommez, I. Hristova, G. Iarygin, A. Ivanilov, A. Izotov,

References II

H. Jackson, A. Jgoun, R. Kaiser, E. Kinney, A. Kisselev, T. Kobayashi, N. Koch, H. Kolster, M. Kopytin, V. Korotkov, V. Kozlov, B. Krauss, V. Krivokhijine, L. Lagamba, L. Lapikás, A. Laziev, P. Lenisa, P. Liebing, L. Linden-Levy, W. Lorenzon, H. Lu, J. Lu, S. Lu, B.-Q. Ma, B. Maiheu, N. Makins, Y. Mao, B. Marianski, H. Marukyan, V. Mexner, N. Meyners, R. Mussa, O. Mikloukho, C. Miller, Y. Miyachi, V. Muccifora, A. Nagaitsev, E. Nappi, Y. Naryshkin, A. Nass, M. Negodaev, W.-D. Nowak, K. Oganessyan, H. Ohsuga, A. Osborne, N. Pickert, D. Potterveld, M. Raithel, D. Reggiani, P. Reimer, A. Reischl, A. Reolon, C. Riedl, K. Rith, G. Rosner, A. Rostomyan, L. Rubacek, J. Rubin, D. Ryckbosch, Y. Salomatin, I. Sanjiev, I. Savin, C. Schill, G. Schnell, K. Schüler, J. Seele, R. Seidl, B. Seitz, R. Shanidze, C. Shearer, T.-A. Shibata, V. Shutov, K. Sinram, W. Sommer, M. Stancari, M. Statera, E. Steffens, J. Steijger, H. Stenzel, J. Stewart, F. Stinzing, P. Tait, H. Tanaka, S. Taroian, B. Tchuiko, A. Terkulov, A. Trzcinski, M. Tytgat, A. Vandenbroucke, P. van der Nat, G. van der Steenhoven, Y. van Haarlem, M. Vetterli, V. Vikhrov, M. Vincter, C. Vogel, J. Volmer, S. Wang, J. Wendland, J. Wilbert, T. Wise, G. Ybeles Smit, Y. Ye, Z. Ye, S. Yen,

References III

B. Zihlmann, and P. Zupranski, "The hermes polarized hydrogen and deuterium gas target in the hera electron storage ring," *Nuclear Instruments and Methods in Physics Research Section A: Accelerators, Spectrometers, Detectors and Associated Equipment*, vol. 540, no. 1, pp. 68–101, 2005.

[3] N. Ramsey, *Molecular Beams*. Oxford University Press, 1956.

[4] F. Willeke and J. Beebe-Wang, "Electron ion collider conceptual design report 2021,"

[5] P. Blümler and H. Soltner, "Practical Concepts for Design, Construction and Application of Halbach Magnets in Magnetic Resonance," *Applied Magnetic Resonance*, vol. 54, pp. 1701–1739, Dec 2023.

[6] H. Soltner and P. Blümler, "Dipolar halbach magnet stacks made from identically shaped permanent magnets for magnetic resonance," *Concepts in Magnetic Resonance Part A*, vol. 36A, no. 4, pp. 211–222, 2010, https://onlinelibrary.wiley.com/doi/pdf/10.1002/cmr.a.20165.

References IV

[7] H. Raich and P. Blümler, "Design and construction of a dipolar halbach array with a homogeneous field from identical bar magnets: Nmr mandhalas," *Concepts in Magnetic Resonance Part B: Magnetic Resonance Engineering*, vol. 23B, no. 1, pp. 16–25, 2004, https://onlinelibrary.wiley.com/doi/pdf/10.1002/cmr.b.20018.

[8] W. Haeberli, "Sources of polarized ions," *Ann. Rev. Nucl. Part. Sci.*, vol. 17, pp. 373–426, 1967.

Spare slides

Critical field for hydrogen hyperfine splitting I

Zeeman region:

- magnetic flux density at which energy separation between different hyperfine levels becomes comparable to Zeeman splitting.
- referred to as *critical magnetic field* or *Breit-Rabi field* B_c
- Breit-Rabi formula (energy levels of hydrogen atom in external magnetic field:

$$E_{F,m_F} = -\frac{E_{\mathrm{hfs}}}{2(2I+1)} + g_J \mu_B m_J B \pm \frac{E_{\mathrm{hfs}}}{2}\sqrt{1+\frac{2m_F x}{F}+x^2}\,, \text{where} \qquad (21)$$

- E_{hfs} is hyperfine splitting energy
- I is nuclear spin (for H, $I = \frac{1}{2}$)
- g_J is Landé g-factor
- μ_B is Bohr magneton
- m_J is magnetic quantum number
- m_F is total angular momentum quantum number
- $x = \frac{g_J \mu_B B}{E_{\mathrm{hfs}}}$
- $F = I + J$ is total angular momentum (for H, $J = \frac{1}{2}$)

Critical field for hydrogen hyperfine splitting II

For H:

- hyperfine splitting energy E_{hfs} (1420 MHz):

$$E_{\mathrm{hfs}} \approx 5.874 \times 10^{-6}\,\mathrm{eV} \tag{22}$$

- Critical field B_c is when Zeeman energy $g_J \mu_B B$ is comparable to E_{hfs}. With $g_J \mu_B B_c \approx E_{\mathrm{hfs}}$, we get:

$$B_c \approx \frac{E_{\mathrm{hfs}}}{g_J \mu_B} \tag{23}$$

- For H, $g_J \approx 2$ (approximately for electron), and $\mu_B \approx 5.788 \times 10^{-5}\,\mathrm{eV/T}$. Thus,

$$B_c \approx \frac{5.874 \times 10^{-6}\,\mathrm{eV}}{2 \times 5.788 \times 10^{-5}\,\mathrm{eV/T}} \approx 50.7\,\mathrm{mT} \tag{24}$$

Polarization of H as function of magnetic field I

Polarization of individual hfs of H (see, e.g., [8])

- $$a = \frac{x}{\sqrt{1+x^2}}\,, \quad \text{where} \quad x = \frac{B}{B_c} \tag{25}$$

so that

$$\begin{aligned} P_{|1\rangle} &= +1\,, & P_{|2\rangle} &= -a\,, \\ P_{|3\rangle} &= -1\,, & P_{|4\rangle} &= +a \end{aligned} \tag{26}$$